

We thank the reviewer for the huge effort dedicated to the improvement of our paper. We address the detailed comments below. The comments of the reviewer are in blue, the answers are in green and the relevant changes in the text are in black.

This is the 4th review of the present study by Kozachek et al.: Large-scale drivers of Caucasus climate variability in meteorological records and Mt Elbrus ice cores. I also reviewed the 2nd and 3rd version. The manuscript has constantly improved with each version. I appreciate the efforts by the authors to address the issues raised in the previous reviews. By now, almost all of these points are convincingly considered. Still, the splitting of the data into seasons seems not quite settled yet, a concern also raised by another reviewer. Further, there are a few explanations provided in the authors' response which did not find their way into the manuscript text although they seem important for clarity. Unfortunately, again the wrong dataset is plotted in one of the figure panels. Although such repeated, basic oversights do not help, I take the authors by their word, trusting that no comparable mistakes happened when evaluating the datasets. The language has improved significantly between the previous and this version, but nevertheless I encourage the authors to take advantage of the language editing offered by the journal. In conclusion, if the (generally) minor points in the comments below can be addressed, I think the manuscript could be accepted for publication.

#### **Detailed comments:**

**L178-181** This is still unclear. If the maximum values are always assigned to July and the minimum values are always assigned to January, how can in some occasions minimum values suddenly become assigned to summer and maximum values to winter? This makes no sense. The approach described above is similar to the one in Vinther et al. (2010) and the underlying assumption for such an approach (max=summer, min=winter) is 50% winter and summer accumulation. The boundary between summer and winter is then defined by the middle between these two extreme (depth scale in m w.e.). This approach to split the record into seasonal data (cold, warm) allows comparison with the meteorological data separated into the seasons in the way described in the manuscript. However, the way I understand the approach described in the present version it seems the minima and maxima are always assigned to the middle of the respective season (cold and warm, respectively). But still I cannot imagine why minima/maxima suddenly should become assigned to winter/summer. In any case the described approach (or my interpretation of its description) contains two additional assumptions: (1) the month of lowest (highest) T is always in the mid-season and (2) this has not changed over the investigated period. Both points and their potential consequences for the analysis due to the fact that both introduce additional uncertainty should in this case be discussed. With the station T data at hand it is easily possible to investigate these two assumptions. Therefore, e.g. plot the months with lowest/highest T against time. The results should show the months of most extreme temperatures to (1) lie in the middle of the respective season and (2) the months when these minima/maxima were observed did not change over time. Actually (1) has been shown to be valid by the data presented in manuscript Fig. 4. Please explain your approach accordingly or adjust your methodology following the description in Vinther et

al. (2010). The subsequent evaluation of the data (correlation analysis etc.) and its interpretation should then also be revised.

Yes, these two assumptions were used and they are confirmed by the weather observations. The middle of the warm season is the end of July – beginning of August. During the whole period of observation the maximum temperature was observed outside this period in 1969 only, when the maximum temperature was in June. In the cold season the middle of the season is the end of January – beginning of February. The minimum values of temperature were observed outside this period in 1971, 1985, 1995, and 1997. We therefore consider this assumption being valid for the whole period of time discussed in the paper.

In some occasions minimum values could become assigned to summer and maximum values to winter. That happened in the cases when minima and maxima were close to each other but the previous extreme was far away. Thus, it was impossible to keep the methodology as in these cases the extreme value was obviously not at the middle of the season. It worth being noticed that these years are not the years listed in the previous paragraph. As these cases were observed just six times over the whole period investigated, we removed this additional explanation from the text to avoid confusion.

We assume that the maximum value of  $\delta^{18}\text{O}$  in the annual cycle corresponds to July and the minimum value corresponds to January and put the border so that these extreme values are in the middle of a season. This method is based on two assumptions. Firstly, the months of the most extreme temperature lie in the middle of the corresponding season. Secondly, the validity of the first assumption does not change over time. Both assumptions are confirmed with the weather observations in the region. The middle of the warm season is the end of July-beginning of August. During the whole period of observation the maximum temperature was observed outside this period in 1969 only, when the maximum temperature was in June. In the cold season the middle of the season is the end of January–beginning of February. The minimum values of temperature were observed outside this period in 1971, 1985, 1995, and 1997. We therefore consider the first assumption being valid for the whole period of time discussed in the paper. We also used ammonium concentration as an independent marker, using criteria described on (Mikhaleenko et al., 2015).

**L168-170** With the additional information about the two absolute time markers (1963 and 1912) now provided in L163-164, a lot about the dating was clarified including the reasoning behind the selection of the 100 year period. Clearly, this period was not selected because of the beauty of the number 100 as suggested in the authors' response, but rather because at that depth the age scale is well defined by the 1912 time horizon. I thus suggest, adding this relevant information to the manuscript along the lines: "This period has been chosen because at this depth, the age scale is well defined by the time horizon found slightly below (Katmai 1912) resulting in a relatively small dating uncertainty of  $\pm 2$  years, and because of the availability of other records such as local meteorological observations."

Added

This period has been chosen because at this depth, the age scale is well defined by the time horizon found slightly below (Katmai 1912) resulting in a relatively small dating uncertainty of  $\pm 2$  years, and because of the availability of other records such as local meteorological observations

**L279-280 and Fig. 8** Is the uncertainty of the defined lapse rate (not indicated in Fig. S3) propagated? In any case, the upper panel (annual means) looks very much the same as in the previous version 4. Please check if the correct dataset is plotted and include the lines indicating the standard deviation across the individual records.

We added the uncertainty of the lapse rate to the Fig. S3, and the standard deviation to the Fig.8. The uncertainty of the lapse rate has a seasonal cycle. It is higher in DJF ( $\pm 0.2$  °C/km) and lower in JJA ( $\pm 0.1$  °C/km). The dataset in Fig.8 has been checked, it is correct.

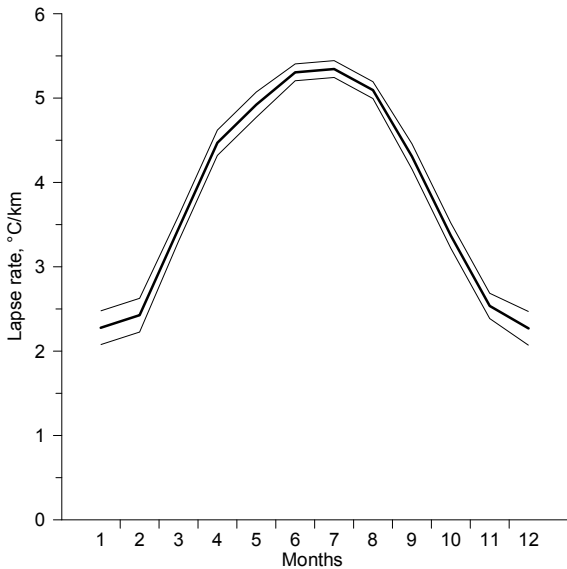


Fig. S3: Calculated monthly mean lapse rate, based on available regional meteorological data for the 1966-1990 period. Thin lines show the uncertainty of the lapse rate estimation.

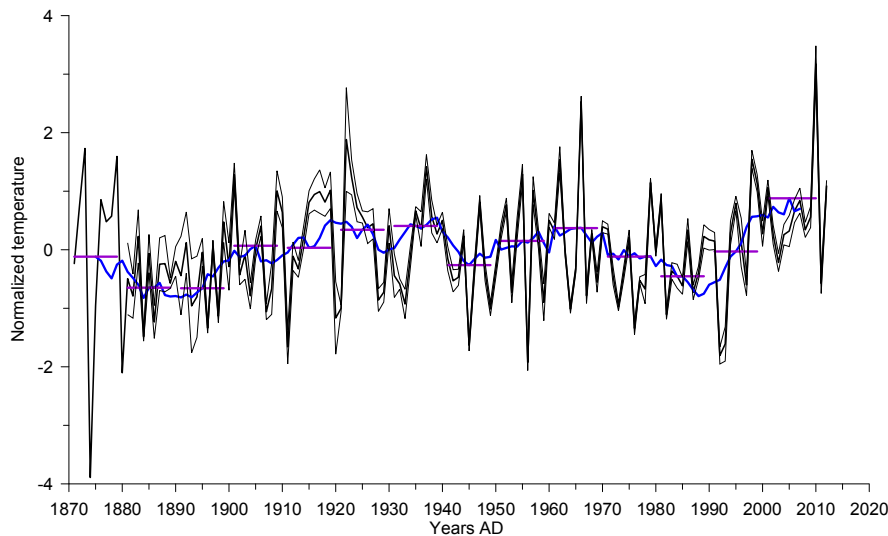
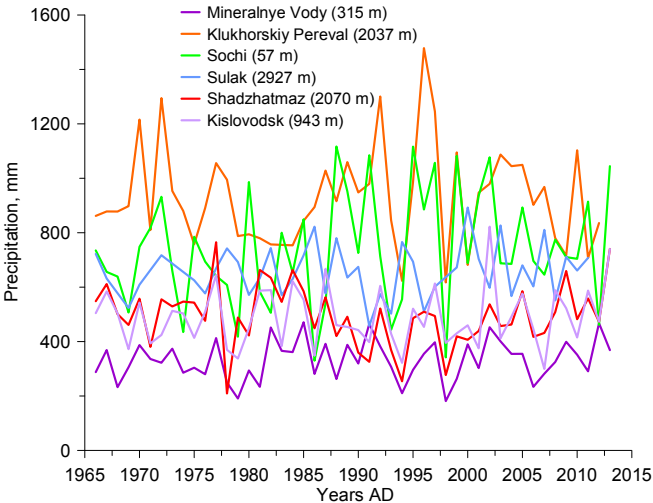


Fig. 8. Normalized regional temperature record based on meteorological data, with respect to the reference period 1966-1990, expressed as annual anomalies ( $^{\circ}\text{C}$ ). The thin lines illustrate the standard deviation across the individual records after accounting for the lapse rate from Fig. S3, the blue line shows 10 year running mean, and the horizontal purple line demonstrates the decadal mean value. The upper panel shows the annual means, the middle panel shows the warm season, and the lower panel shows the cold season

**L280-284 (and Fig. S4)** As suggested, Fig. S4 has now been updated so that it is now consistent with the manuscript text. When now also adding the information about the station altitude to the figure legend, it becomes visually obvious that precipitation variability and particularly for the cold season precipitation amount has a strong altitude effect. With this, the choice to only use the two high altitude stations for precipitation data is clarified. The according text should be added to the manuscript. Therefore, please add altitudes to the legends in Fig. S4 and adjust the text along the lines: “All the precipitation data available for this region since 1966 is shown in fig. S4. Because of the obvious altitude dependence of both precipitation variability and precipitation amount (particularly for the cold season) only the data from the two high altitude stations Klukhorskiy Pereval (???? m asl.) and Mineralnye Vody (???? m asl.) were used for the calculations here. The two stations are further representative for stations with and without a prominent seasonal cycle (Mineralnye Vody and Klukhorskiy Pereval, respectively).”

We added the altitude to the Fig. S4. We disagree with the assumption that these stations were chosen because of their high-altitude position. The Mineralnye Vody station is situated at the altitude of 315 m a.s.l. The reason for the choice of Mineralnye Vody station is the uninterrupted record for the whole period of observation. Because of relatively sparse weather observations, it is difficult to estimate the

126 altitude effect on the precipitation rate. For example, at Sulak, the highest station in the region, the  
127 precipitation rate is not the highest because of the influence of continentality. It is also an orographic  
128 effect that influence the precipitation rate. Stations situated to the South from the Caucasus receive  
129 several times more precipitation than those on the Northern slope. The precipitation rate at any of the  
130 stations is the combination of altitude, continental and orographic effects. It is difficult to calculate the  
131 influence of each of these factors.  
132



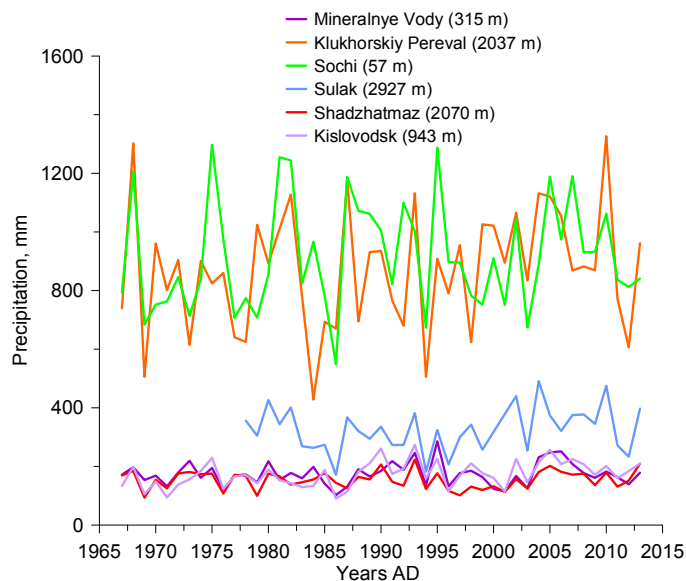


Fig. S4: Precipitation rate in warm season (upper panel) and in cold season (lower panel). Numbers in brackets indicate the altitude of the station above the sea level.

**L437-438** It is unclear for what season NAO is correlated with regional temperature. I suggest changing to: “For the cold season, the ice core d18O record shows...”

Changed

For the cold season, the ice core d18O record shows a positive correlation with the NAO index ( $r = 0.41$ ),...

**Fig. 7** There are only 11 increments for the 12 months which is confusing. To be consistent within the manuscript and with the commonly used way for display, please adjust the x-axis scale similar to manuscript Fig. 4.

Changed

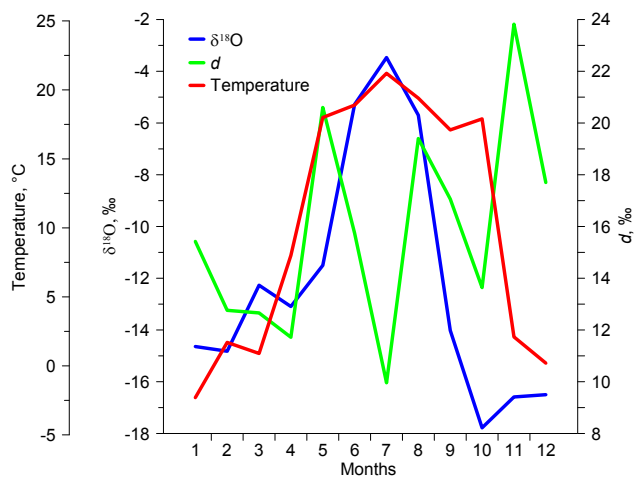


**Fig. 9** Even though the temperature record in this figure (and in Fig. 10) is now at least plotted on the correct age scale, it is still not correct. In the lowermost panel, not d18O is plotted but normalized temperature (most obvious by the y-axis scale). Please correct.

Fig. 9 has been corrected

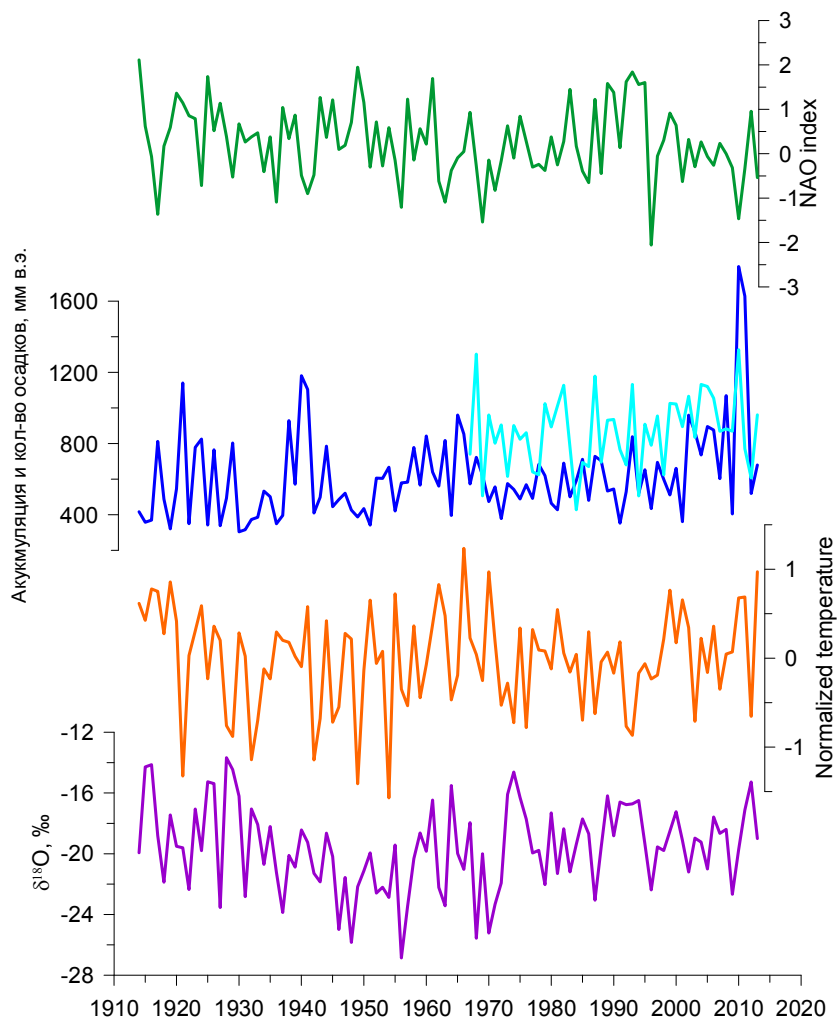


**Table 4 (and according sections in the text)** Although in this version, the normalized temperatures are again used for the correlation analysis as it was suggested, none of the correlation coefficients changed. I do not expect extreme changes but at least some considering the fact that in the previous version only the station data from Klukhorskiy Pereval and Mineralnye Vody was used. Further, for the field in the upper left corner, annual means - T vs d18O – the value of 0.16 (n=100) is not significant and should not be bold.

169 Checked and corrected. The same correlation coefficients were obtained due to very close agreement of  
170 temperature changes at all the stations and low uncertainty of the lapse rate calculation.  
171

172 **Language:**

173 When accepted for publication, please take advantage of the language editing service offered by the  
174 journal. One easy fix: in many cases  $\delta^{18}\text{O}$  should be replaced with  $\delta^{18}\text{O}$ .  
175

176 The language has been checked by the native speaker once again. The spelling of  $\delta^{18}\text{O}$  has been  
177 corrected.  
178

179 **Large-scale drivers of Caucasus climate variability in meteorological**  
180 **records and Mt Elbrus ice cores**  
181

182 Anna Kozachek<sup>1,2,3</sup>, Vladimir Mikhlenko<sup>2</sup>, Valérie Masson-Delmotte<sup>3</sup>, Alexey Ekaykin<sup>1,4</sup>, Patrick  
183 Ginot<sup>5,6</sup>, Stanislav Kutuzov<sup>2</sup>, Michel Legrand<sup>5</sup>, Vladimir Lipenkov<sup>1</sup>, Susanne Preunkert<sup>5</sup>

- 184  
185 1. Climate and Environmental Research Laboratory, Arctic and Antarctic Research Institute, St Petersburg, 199397, Russia  
186 2. Institute of Geography, Russian Academy of Sciences, Moscow, 119017, Russia  
187 3. Laboratoire des Sciences du Climat et de l'Environnement, CEA/CNRS/UVSQ/IPSL, Gif-sur-Yvette, 91191, France  
188 4. Institute of Earth Sciences, St Petersburg State University, St Petersburg, 199178, Russia  
189 5. Laboratoire de Glaciologie et Géophysique de l'Environnement, CNRS/UGA, Grenoble, 38400, France  
190 6. Observatoire des Sciences de l'Univers de Grenoble, IRD/UGA/CNRS, Grenoble, 38400, France

191  
192 *Correspondence to:* Anna Kozachek (kozachek@aari.ru)  
193

194 **Abstract**  
195

196 A 181.8 m ice core was recovered from a borehole drilled into bedrock on the western plateau of Mt Elbrus (43°20'53.9'' N,  
197 42°25'36.0'' E; 5115 m a.s.l.) in the Caucasus, Russia, in 2009 (Mikhlenko et al., 2015). Here, we report on the results of  
198 the water stable isotope composition from this ice core with additional data from the shallow cores. The distinct seasonal  
199 cycle of the isotopic composition allows dating by annual layer counting. Dating has been performed for the upper 126 m of  
200 the deep core combined with 20 m from the shallow cores. The whole record covers 100 years, from 2013 back to 1914. Due  
201 to the high accumulation rate (1380 mm w.e. per year) and limited melting we obtained isotopic composition and  
202 accumulation rate records with seasonal resolution. These values were compared with available meteorological data from 13  
203 weather stations in the region, and also with atmosphere circulation indices, back-trajectory calculations and GNIP data in  
204 order to decipher the drivers of accumulation and ice core isotopic composition in the Caucasus region. In the warm season  
205 (May-October) the isotopic composition depends on local temperatures, but the correlation is not persistent over time, while  
206 in the cold season (November–April), atmospheric circulation is the predominant driver of the ice core's isotopic  
207 composition. The snow accumulation rate correlates well with the precipitation rate in the region all year round, which made  
208 it possible to reconstruct and expand the precipitation record at the Caucasus highlands from 1914 till 1966, when reliable  
209 meteorological observations of precipitation at high elevation began.

210  
211 **1 Introduction**  
212

213 Large-scale modes of variability such as the NAO (North Atlantic Oscillation) are known to influence European climate  
214 variability (see review in Panagiotopoulos et al., 2002). However, most studies of large-scale drivers of European climate  
215 change have been focused on low elevation instrumental records from weather stations, and there is very limited information

about climate variability at high altitudes, and about differences in climate variability and trends at different elevations (EDW research group, 2015). Such differences were calculated in many mountain regions (EDW research group, 2015), except for the Caucasus, due to the lack of high elevation instrumental observations in this region.

The Caucasus is located southwards of the East European Plain. It is a high mountain region, with typical elevations of 3200-3500 m a.s.l., and with the highest point reaching 5642 m for Elbrus. The Main Caucasus Ridge acts as a barrier between subtropical and temperate mid-latitude climates, as observed for other high mountain regions such as the Himalaya. As in other mountain regions, there is a lack of high elevation meteorological records in the Caucasus. Moreover, existing records are relatively short: for example, reliable Caucasus precipitation measurements only started in 1966. Improved spatio-temporal coverage is required to investigate internal variability, to explore trends and spatial differences, and to evaluate the skills of atmospheric models providing atmospheric analysis products where no meteorological data are assimilated.

Measurements of the stable isotope composition of water, and annual accumulation rates in mid to high latitude ice cores are widely used proxies to estimate past temperature and precipitation rate changes. In many high mountain regions such as the Caucasus, and for elevations situated above the tree line, ice core data provides the only source of detailed information to document past climate changes, complementing punctual information retrieved from changes in glacier extent and recent glacier mass balance. For example, a study of the water stable isotope composition of several ice cores obtained in the Alps was recently conducted by Mariani et al. (2014) and the same research in Alaska was performed by Tsushima et al. (2015).

The authors explored the links between the ice cores' isotopic composition, local climate, and large-scale circulation patterns. They found that in mountain regions, the isotopic composition of the ice cores was governed both by local meteorological conditions and by regional and global factors. These studies discussed the complexity of interpreting ice core records from high-altitude glaciers due to the potential bias from post-depositional processes and frequent changes in the origin of moisture sources. For instance, even in areas without any seasonal melt, accumulation is the net effect of precipitation, sublimation, and wind erosion processes, and may significantly differ from precipitation. Water stable isotope records are in mid to high latitudes physically related to condensation temperature through distillation processes (Dansgaard, 1964), but the climate signal is archived through the snowfall deposition and post-deposition processes. One important artefact lies in the intermittency of precipitation, and the covariance between condensation temperature and precipitation, which may bias the climate record towards one season, or towards one particular weather regime, challenging an interpretation in terms of annual mean temperature (Persson et al., 2011). Moreover, water stable isotopes are integrated tracers of all phase changes occurring from evaporation to mountain condensation, and are also affected by non-local processes related to evaporation characteristics, or shifts in initial moisture sources. Such processes have the potential to alter the validity of an interpretation of the proxy record in terms of local, annual mean, or precipitation-weighted temperature. In some regions, isotopic records are more related to hydrological cycles, recycling, or rainout (Aemisegger et al., 2014). Finally, the condensation temperature may also strongly differ from surface air temperature; depending on elevation shifts in e.g. planetary boundary layer or convective activity (see Ekaykin and Lipenkov, 2009 for a review). While these processes make the interpretation of ice core records complex, they do open the possibility that the ice core proxy record may be in fact

more sensitive to large-scale climate variability than punctual precipitation amounts. For instance, Casado et al (2014) have evidenced a strong fingerprint of the NAO in water stable isotope records from central Western Europe and Greenland, either in long instrumental records based on precipitation sampling, in seasonal ice core records, or in atmospheric models including water stable isotopes. The connection of Greenland ice cores' isotopic composition with ~~the~~-atmospheric circulation patterns was studied by Vinther et al. (2003 and 2010). The strong influence of the NAO pattern on the Greenland ice cores' isotopic composition has been discovered and the possibility to use the ice cores data for the reconstruction of the past NAO changes was suggested (Vinther et al., 2003). The authors also revealed the importance of the study of the seasonally resolved ice cores records rather than annual records, as there are different factors governing formation of the isotopic composition of precipitation in warm and in cold seasons (Vinther et al., 2010).

We will now briefly review earlier studies performed on climate variability in the Caucasus area, which have already explored the relationships between regional climate, glacier expansion, and large-scale modes of variability: the NAO (North Atlantic Oscillation), AO (Arctic Oscillation), and NCP (North Sea–Caspian Pattern). For example, Shahgedanova et al. (2005) monitored the mass balance of the Djankuat glacier, situated at an altitude between 2700 and 3900 m a.s.l. While no significant correlation was identified between ~~the~~ accumulation rate and the winter NAO index, the years of high accumulation systematically occurred during winters with a very negative NAO index. Brunetti et al. (2011) explored the influence of the NCP mode on climate in Europe and around the Mediterranean region. They evidenced a negative correlation coefficient of -0.50 between temperature in the Caucasus and the NCP index. Baldini et al. (2008) investigated records of precipitation isotopic composition in Europe from the IAEA/GNIP stations, extrapolating a significant negative correlation between winter precipitation  $\delta^{18}\text{O}$  in the Caucasus region and the NAO index ( $R = -0.50$ ). Casado et al (2013) studied the influence of precipitation intermittency on the relationships between precipitation  $\delta^{18}\text{O}$ , temperature, and the NAO. The influence of the NAO index on European climate and precipitation  $\delta^{18}\text{O}$  appeared more prominent in winter than in summer (Comas-Bru et al., 2016).

Here, we take advantage of the new Elbrus deep ice cores (Mikhalev et al., 2015), and produce the first analysis of water stable isotope and accumulation records. Section 2 introduces the data and methods, with a description of the ice core analyses and age scale, an overview of regional meteorological information, and the source of information for indices of modes of variability. Section 3 presents the results of the comparison and statistical analyses of the relationships between regional climate parameters (temperature and precipitation), Elbrus ice core records, and modes of variability. In section 4, we summarize our key findings and the next steps envisaged to strengthen the climatic interpretation of the Caucasus ice core records.

## 2 Data and methods

### 2.1 Ice core data

284 **2.1.1 Drilling site and drilling campaigns**

285

286 Here, we report on results from the new, deepest ice core from Mt Elbrus, in comparison with results from shallow ice cores.  
287 Deep drilling was performed on the Western Plateau (43°20'53.9" N, 42°25'36.0" E; 5115 m a.s.l.) of Mt Elbrus (fig. 1) in  
288 September 2009, allowing recovery of a 181.8 m long ice core, down to bedrock. The drilling site and the drilling operations  
289 are thoroughly described in Mikhalenko et al. (2015).

290 In order to update the ice core records towards the present-day, and enable a comparison of the measurements with local  
291 meteorological monitoring data, surface drilling operations were repeated at the same place in 2012 (11.5 m long) and in  
292 2013 (20.5 m long). Results are also compared here with previously published isotopic composition data measured along the  
293 22 m shallow ice core drilled at the same place in 2004 which covered the period from 1998 till 2004: (Mikhalenko et al,  
294 2005).

295 In 2014, drilling operations were also successful at the Maili Plateau (Mt Kazbek), at the altitude of 4500 m a.s.l. in 200 km  
296 eastwards from Elbrus (fig. 1), delivering a 20-m ice core. The Kazbek core is shown for purposes of comparison only. A  
297 detailed description of it will be published elsewhere.

298

299 **2.1.2 Sampling process and sampling resolution**

300

301 For the upper and the lower parts of the deep core (0-106 m and 158-181.8 m) and for the shallow firn cores drilled in 2012  
302 and 2013, sampling was performed using classic cutting-melting procedures. For the other depth intervals, melted samples  
303 were extracted from the continuous flow analysis system of LGGE (Grenoble, France), automatically sub-sampled, frozen  
304 and stored in vials for subsequent isotopic analysis. The description of the CFA system will be published elsewhere.

305 The sampling resolution was 15 cm for the upper 16 m of the deep core (see the sketch of the sampling resolution in fig. 2c).

306 It was then increased to 5 cm in order to achieve better resolution, from 16 to 70 m depth and in the bottom part of the core  
307 (158-182 m depth). To ensure 15-20 samples per year, the sampling resolution was increased to 4 cm in the depth range from  
308 70 to 106 m, similar to the sampling resolution of the CFA system (3.7 cm).

309 Samples from the shallow cores drilled in 2012 and 2013 were cut with a resolution of 10 and 5 cm, respectively.

310

311 **2.1.3 Isotopic measurements**

312

313 The methods for the isotopic measurements have been partially discussed in (Mikhalenko et al., 2015). Water stable isotope  
314 ratios ( $\delta^{18}\text{O}$  and  $\delta\text{D}$ ) were measured at the Climate and Environmental Research Laboratory (CERL) at the Arctic and  
315 Antarctic Research Institute (St Petersburg, Russia), using a Picarro L2120-i analyzer. Each sample was measured once.  
316 Sequences of measurements included the injection of 5 samples, followed by the injection of an internal laboratory standard  
317 with an isotopic value close to that of the samples. We also repeated the measurements of about 10% of all the samples in

order to calculate the analytical precision: 0.06‰ for  $\delta^{18}\text{O}$  and 0.30‰ for  $\delta\text{D}$ . The depth profile of  $\delta^{18}\text{O}$  (Mikhalenko et al., 2015; Kozachek et al., 2015) and of the deuterium excess ( $d = \delta\text{D} - 8 \cdot \delta^{18}\text{O}$ ) are shown in fig. 2.

Moreover, 600 samples from the depth interval from 23 to 35 m were measured in the Laboratory of Isotope Hydrology of the IAEA (Vienna, Austria). The two records are highly correlated ( $r=0.99$ ,  $p < 0.05$ ) for both isotopes (Figure S2b) with a systematic offset of 0.2 ‰ for  $\delta^{18}\text{O}$  and 1 ‰ for  $\delta\text{D}$ . The records of the second order parameter deuterium excess are also significantly correlated ( $r=0.65$ ,  $p < 0.05$ ) without any specific trend or systematic offset. This inter-laboratory comparison demonstrates the high quality of the isotopic measurements performed in CERL.

We also stress the close overlap of the upper part of the profiles of the water stable isotope records versus depth from the different cores drilled in 2009, 2012 and 2013 (Fig. S2a). Based on this close agreement within the different shallow firm cores, we decided to calculate a stack record for the period from 1914 till 2013, which is used for dating hereafter.

In the depth interval from 100 to 106 m depth, we also have an overlap of samples obtained with classic cutting method and CFA method described above, without any significant difference (Fig. S2c), again allowing us to combine the two records into one stack record.

#### 2.1.4 Dating

The chronology is based on the identification of annual layers. These are prominent in  $\delta^{18}\text{O}$  with the average seasonal amplitude of 20 ‰. For annual mean values we calculated averages of  $\delta^{18}\text{O}$  from one minimum of this parameter to another one as well as from one maximum to another. As we found no significant differences between the records obtained with two ways of year allocation we used minimum to minimum dating as a more common method. We compared annual layer counting performed independently using the seasonal cycles in the isotopic composition and the ammonium concentration. The discrepancy between two independent chronologies is 2 years at a depth of 126 m. We used the dating based on the isotopic composition data in this paper. This dating is also best fit for the correlation analysis with the meteorological data. For the estimation of the dating uncertainties we used the absolute age markers. These markers are the tritium peak in 1963 and the sulfate peak in 1912 which corresponds to the Katmai eruption (Mikhalenko et al., 2015). The comparison of different dating methods on age control points shows that the overall error of our timescale at these two depth levels does not exceed  $\pm 2$  years which means that independent dating uncertainties should compensate each other at this points

Hereafter, we focus our analysis on one hundred years, from 1914 till 2013, which corresponds to the total of 140 m of the ice thickness studied here (the 15 m covered by the shallow cores plus the 126 m covered by the deep ice core). This period has been chosen because at this depth, the age scale is well defined by the time horizon found slightly below (Katmai 1912) resulting in a relatively small dating uncertainty of  $\pm 2$  years, and because of the availability of other records such as local meteorological observations~~This period has been chosen because of the relatively small dating uncertainty ( $\pm 2$  years) and the availability of other records such as local meteorological observations.~~ In the bottom part of the core the cycles in the isotopic composition are less prominent and dating becomes less reliable, leading to a significant increase in uncertainty. The

isotopic composition of that part of the core will be discussed elsewhere. In meteorological data we used average values from January to December of each year for the comparison with the annual means of ice cores parameter.

For warm and cold seasons allocation, we used a method adapted slightly from (Vinther et al., 2010). The original method requires ascribing of an equal accumulation rate for the warm and cold season of each year. Basically we used the same approach as there is an obvious seasonal cycle of  $\delta^{18}\text{O}$  which is coherent with the seasonal cycle of temperature in the region.

~~We assume that the maximum value of  $\delta^{18}\text{O}$  in the annual cycle corresponds to July and the minimum value corresponds to January and put the border so that these extreme values are in the middle of a season. This method is based on two assumptions. Firstly, the months of the most extreme temperature lie in the middle of the corresponding season. Secondly, the validity of the first assumption does not change over time. Both assumptions are confirmed with the weather observations in the region. The middle of the warm season is the end of July-beginning of August. During the whole period of observation the maximum temperature was observed outside this period in 1969 only, when the maximum temperature was in June. In the cold season the middle of the season is the end of January-beginning of February. The minimum values of temperature were observed outside this period in 1971, 1985, 1995, and 1997. We therefore consider the first assumption being valid for the whole period of time discussed in the paper. We therefore assume that the maximum value of  $\delta^{18}\text{O}$  in the annual cycle corresponds to July and the minimum value corresponds to January and put the border so that these extreme values are in the middle of a season. However, there were several situations (six for the whole ice core record) when this approach could potentially lead to assign minimum values to summer and maximum to winter. In order to avoid this problem we used the middle point between minimum and maximum as a border between seasons in such cases.~~

We also used ammonium concentration as an independent marker, using criteria described on (Mikhaleiko et al., 2015). For equivocal situations, we also used additional data: melt layers and dust layers (used to identify the warm season) (Kutuzov et al., 2013) as well as succinic acid concentration data that also have seasonal variations (Mikhaleiko et al., 2015).

Figure 3 illustrates the identification of seasons using the isotopic composition seasonal cycle. In the meteorological data we used the period from November to April for the cold season and May to October for the warm season.

There some gaps in the isotopic composition data that came from technical problems during the drilling operations and the process of analysis. The drilling problems are described in (Mikhaleiko et al., 2015). The biggest gap appears at the depth of 31.3 and 32.1 m. A piece of the core was lost during the drilling operations. This part is covered by the bottom part of the 2004 core where the sampling resolution was 50 cm. It is evident that two seasons (one warm and one cold) are partially missing. We did not use these values for the correlation analysis because of the large uncertainty of the seasonal values calculations in this case. In case of a missing sample we considered its isotopic value to be the average between the two neighboring samples. For a detailed description of the raw isotopic data and annual layers allocation for the upper 106 m of the core, please refer to Mikhaleiko et al. (2015). Mean annual and seasonal values of  $\delta^{18}\text{O}$  and  $d$  obtained as a result of the dating are shown in fig. 5 and 6 respectively.

The annual accumulation rate is calculated as the thickness of the seasonal layer, multiplied by the layer density using the density profile from Mikhaleiko et al. (2015), and corrected for layer thinning using the Nye model (Nye, 1963; Dansgaard

and Johnsen, 1969), with the following parameters: accumulation rate 1.583 m of ice equivalent, pore close-off depth = 55 m (Mikhalenko et al., 2015).

**2.1.5 Diffusion of stable isotopes**

We calculated the potential influence of diffusion on the stable isotopes record according to [the](#) (Johnsen, 2000) model. We used the following parameters for the calculation: Our calculation showed that the seasonal amplitude of  $\delta^{18}\text{O}$  variations could be 10-20% less because of the diffusion (Mikhalenko et al., 2015). If it was the case we would observe a decreasing of  $\delta^{18}\text{O}$  maxima and increasing of minima with depth. Moreover we would find a positive correlation between layer thickness and a seasonal amplitude of  $\delta^{18}\text{O}$ . These features have not been found in the ice core data. The correlation coefficient between seasonal amplitude and accumulation rate is -0.10 and is statistically insignificant. There is also no statistically significant trend in the seasonal amplitude; the seasonal amplitude varies stochastically from 10 to 25 ‰. The maximum value observed in 1984 and the minimum in 1925. We therefore consider that the diffusion does not sufficiently influence the isotopic composition record in the upper 126 m of the ice core. At the bottom part of the core (e.g. at a depth of 180 m) the annual cycle of  $\delta^{18}\text{O}$  should have an amplitude of 4 ‰ which is detectable but the length of the cycle should be less than 1 cm. As the  $d$  annual cycle is not prominent we cannot use the method based on the discrepancy between the  $\delta^{18}\text{O}$  and  $d$  cycles. Thus, for obtaining climatic information from the bottom part of the core, a very high sampling resolution is required.

**2.2 Meteorological data**

We used the daily meteorological data (precipitation rate and mean daily temperature) from several weather stations around the drilling site (see map in Fig. 1 and Table 1) for comparison with the ice core data. We also investigated records of precipitation isotopic composition based on monthly sampling, performed at three stations to the south of the Caucasus within the WMO-IAEA Global Network of Isotopes in Precipitation (GNIP) program (Table 1).

For comparison we used the NCEP/NCAR reanalysis temperature data (Kalnay et al., 1996) for the 500 mbar level which corresponds to the drilling site altitude. Two different models were used to calculate back trajectories: FLEXPART (Forster et al., 2007, Stohl et al., 2009), HYSPLIT (Draxler, 1999, Stein et al., 2015, Rolph, 2016). The LMDZiso model was used to estimate the precipitation isotopic composition at the drilling site (Risi et al., 2010).

**2.3. Circulation indices**

Circulation of the atmosphere sufficiently influences isotopic composition of the ice cores (Casado et al., 2013 and references therein). Atmospheric circulation is quantitatively characterized by circulation indices. In this research we used three indices: NAO, AO, and NCP, that are widely used to characterize European climate (Jones et al., 2003, Thompson and Wallace, 2001, Brunetti et al., 2011 and references therein). Time span and references for the indices are presented in table 1.

NAO (North-Atlantic Oscillation) characterizes the type of circulation in Europe, strength of Azores maximum and Icelandic minimum. The positive values of the NAO index correspond to the lower than usual value of the atmospheric pressure in Iceland and the higher than usual value of atmospheric pressure at Azores. The negative index corresponds to the less prominent centres of action in the Northern Hemisphere. Usually this index is calculated as a difference of atmospheric pressure measured at Reykjavik and Lisbon, Ponta Delgada or Gibraltar. Here we used data from (Vinther et al., 2003 and <https://crudata.uea.ac.uk/~timo/datapages/naoi.htm>) that were calculated using data from Gibraltar station. The negative NAO leads to an increase in the precipitation rate in Southern Europe, while a positive NAO leads to an increase in the precipitation rate in Northern Europe (Hurrell, 1995, Jones et al., 2003, Vinther et al., 2003).

The Arctic Oscillation index (AO) is also a characteristic of the Northern Hemisphere circulation. It is used to analyze climatic variability with periods longer than 10 years. It is calculated as EOF of 500 hPa surface. Negative values correspond to high pressure at the Pole and the cooling of Europe, while positive values correspond to low pressure at the Pole and the drying of the Mediterranean (Thompson and Wallace, 2001). We used AO data from NOAA (<http://www.cpc.ncep.noaa.gov/products/precip/CWlink/>).

The NCP (North-Sea Caspian Pattern) index is less widely used, though it was proved that it is convenient to use it in Mediterranean climate studies (Kutiel et al., 1997; Brunetti et al., 2011). The index is calculated as a normalized difference of geopotential heights between the Caspian and Northern seas. Positive values correspond to stronger meridional circulation in Europe and lower summer temperatures, while negative values reflect the strengthening of zonal circulation and higher summer temperatures in Europe (Brunetti et al., 2011). We used NCP data from NOAA (<http://www.cpc.ncep.noaa.gov/products/precip/CWlink/>).

### 3 Results

#### 3.1 Regional climate

The main peculiarity of the drilling site is its location on the border between subtropical and temperate climatic zones (Volodicheva, 2004). Back-trajectory calculations show that the drilling site is characterized by remarkable seasonal differences in the locations of moisture sources. In winter, the origin of air masses varies from the Mediterranean to the North Atlantic. In summer, local moisture sources from the surrounding continents or from the Black Sea are predominant (see fig. S1 for examples).

Meteorological data depict large regional variations in the seasonal cycle of precipitation. To the south of the Caucasus, there is no distinct seasonal cycle (Fig. 4a), showing the climatology for the Klukhorsky Pereval station. In fact, the Klukhorsky Pereval station is situated north of the Main ridge, but in terms of the seasonal cycle of precipitation it undoubtedly belongs to the southern group. However, we are nevertheless using this station as an example because of the uninterrupted record of temperature and precipitation for the 1966-1990 period. By contrast, the north of the Caucasus is marked by a distinct

seasonality in precipitation amounts, which are maximum in summer and minimum in winter (Fig. 4b), showing the climatology for the Mineralnye Vody station. More examples of the Caucasus weather stations climatologies are given in (Mikhaleiko et al., 2015). Moreover, the annual precipitation rate to the south of the Caucasus is much higher than to the north. For example, the typical annual precipitation rate to the north of the Caucasus at an altitude close to sea level is 500 mm per year, while to the south of the Caucasus at the same altitude it is about 1500 mm. The amount of precipitation in the region is affected by the altitude and the distance from the sea shore.

The seasonal changes of temperature appear uniform throughout the region surrounding the Caucasus, with the warmest conditions observed in summer and the coldest observed in winter. The seasonal amplitude depends on the distance from the sea and the mean annual temperature depends on the altitude. The average regional lapse rate was calculated using the available meteorological data. We used the data from all the stations for the calculation. The lapse rate is lowest in December-February (2.3°C per 1000 m) and highest (5.2 °C per 1000 m) in June-August (Fig. S3).

Based on the lapse rate, we calculated the temperature at the drilling site taking into account its seasonal variability shown on the fig. S3. This record was used for the estimation of the  $\delta^{18}\text{O}$ -temperature relationship. For the comparison with the ice core data we used the dataset of the normalized temperature data. Normalized temperature time series were calculated for each station for each season or for the whole year, and results were then averaged (fig. 8). For precipitation data, available in this region since 1966, we show all the data (fig. S4), while in the calculations we used data from Klukhorskii Pereval station as an example of a station without a seasonal cycle, and from Mineralnye Vody station as an example of those one with a prominent cycle. More examples of annual variations of temperature and precipitation at the Caucasus meteorological stations can be found in (Shahgedanova et al., 2014) and (Tielidze, 2016). At our drilling site, an automatic weather station (AWS) provided in situ measurements for the period from August 2007 till January 2008. The day to day variations of temperature at low elevation weather stations and at the AWS are coherent for the whole period of the AWS work (Mikhaleiko et al., 2015).

We also compared the data from meteorological stations with the NCEP reanalysis (Kalnay et al., 1996) outputs (not shown) for the 500 mbar level. Despite the difference in absolute values on a daily scale when compared with the AWS data (the difference is random and varies from -1 to 1 °C), the observed regional data and reanalysis data have the same month to month variability. The maximum daily mean temperature at the drilling site according to the reanalysis data was -1.3°C for the whole dataset. The temperature in the glacier at 10m depth, which corresponds to the annual mean temperature at the drilling altitude, is -17°C (Mikhaleiko et al., 2015), the annual mean temperature at the drilling altitude from the NCEP reanalysis is -14 °C, and the same value calculated from meteorological observations and corrected for the lapse rate is -11 °C.

We then investigated long-term trends in the meteorological records. Mean annual temperatures show a significant increase during the last two decades. We also observe higher than average values of mean decadal temperature in 1930-1940. And the beginning of the observations in the region, i.e. the period from 1881 till 1900, was as cold as the 1990s. It is evident that the last 20 years in the warm season were the warmest for the whole observation period (fig. 8), while in the cold season the

recent warming is not unprecedented. For example, cold seasons in the 1960s—1970s were even warmer (fig. 8). Multi-decadal patterns of temperature variations also differ in the late 19<sup>th</sup> century, where negative anomalies are identified in cold season temperature (Fig. 8) but not in warm season temperature (Fig 8). On the other hand in cold season temperatures we can observe lower temperatures at the end of the 19<sup>th</sup> century that ~~ean-might~~ be due to the impact of the volcanic eruptions (Stoffel et al., 2015). We also noted the high temperature values in the 1910s—1920s that are not completely understood. We did not find any trends in the precipitation rate for any of the groups of stations (fig. S4).

A significant anti-correlation is observed between temperature and the NAO index, both in the cold and warm seasons (Table 2, the information about the time series used for the correlation analysis can be found in Table 1). Stronger anti-correlations are identified between temperature and the NCP index, especially in the cold season, as also reported by Brunetti et al. (2011). Relationships with indices of large scale modes of variability are systematically weaker for precipitation, with contradictory results for the south/north Caucasus stack; they appear significant for the NCP in both seasons (Table 2).

GNIP data are only available at low elevation stations. They show a rather uniform distribution of the isotopic composition of precipitation in the region during summer, as well as a gradual depletion of  $\delta^{18}\text{O}$  at higher altitudes in winter. GNIP records are too short and intermittent (one-two years with gaps) to investigate the variability and relationships with the local temperature on an interannual scale. We therefore restrict discussion of GNIP data to seasonal variations. The  $\delta^{18}\text{O}$  and  $\delta\text{D}$  in precipitation have a distinct seasonal cycle with maximum values observed in the warm season (JJA) and minimum values observed in the cold season (DJF). As an example we show the seasonal cycle of  $\delta^{18}\text{O}$  and  $d$  for Bakuriani station in 2009 (fig. 7). This station is the only one in the region for which the whole uninterrupted dataset for one annual cycle is available. The seasonal amplitude of  $\delta^{18}\text{O}$  is about 17 ‰. The slope between  $\delta^{18}\text{O}$  and temperature is 0.32 ‰/°C. The  $d$  variations show no seasonal cycle varying randomly between 10 ‰ and 25 ‰. We found no significant correlation between  $\delta^{18}\text{O}$  and  $d$ .

Climate variability as a driver for glacier variations in the Caucasus has recently been explored by several authors. Elizbarashvili et al. (2013) found the increased frequency of extremely hot months during the 20<sup>th</sup> century, especially over Eastern Georgia, whereas the number of extremely cold months decreased faster in the Eastern than in the Western region. In addition, the highest rates for positive trends of annual mean air temperature can be observed in the Caucasus Mountains. Shahgedanova et al. (2014) evidenced significant glacier recession at the northern slopes of the Caucasus, consistent with increasing air temperature of the ablation season. They report that the most recent decade (2001-2010) was 0.7–0.8 °C warmer than in 1960-1986 at Terskol and Klukhorskyy Pereval stations (see Table 1 for information on stations). However, the warmest decade for JJA was 1951-1960 (Shahgedanova et al., 2014). Tielidze (2016) reports a recent increase in the annual mean temperatures at different elevations in the Georgian Caucasus. The region experienced glacier area loss over the 20<sup>th</sup> century at an average annual rate of 0.4% with a higher rate in eastern Caucasus than in the central and western sections. The analysis of temperature and radiation regime of glaciers at the ablation period has been performed at Elbrus vicinities recently (Toropov et al., 2016). The authors prove that the observed waning of glaciers cannot be explained by ~~an~~ increase ~~of~~ in temperature during the ablation period because of an increase in precipitation during the accumulation period. They

concluded that the main driver of glacier retreat is the increase of the solar radiation balance for 4% for the 2001-2010 period which corresponds to the increase of ablation for 140 mm per ablation season (Toropov et al., 2016).

### 3.2 Ice core records

The comparison of the four cores obtained at the Western Plateau of Elbrus shows similar variations during overlap periods (see Fig. 2S). We therefore calculate a stack record for each season, based on the average value of individual ice cores for the overlapping seasons. The inter-core disagreement is almost negligible (fig. 2S) and can be explained by different sampling resolution.

We note that the shallow ice core from the Maili plateau of Kazbek shows the same mean values of  $\delta^{18}\text{O}$  as the Elbrus ice cores during their overlap period. This is a result of a mutual compensation of  $\delta^{18}\text{O}$  increase due to the lower elevation position (Kazbek drilling site is 500 m lower) and of  $\delta^{18}\text{O}$  decrease because of the continentality effect (Kazbek is 200 km further from the sea). We calculated the continental gradient and lapse rate for  $\delta^{18}\text{O}$  using the data from the GNIP stations in the region that are situated at the lower elevations. The lapse rate is  $-0.25\text{‰}/100\text{ m}$  and continental gradient is  $-0.85\text{‰}/100\text{ km}$ . The mean value of  $\delta^{18}\text{O}$  for the Kazbek ice core should be 1.25‰ more positive because of elevation difference and 1.7‰ more negative due to the continentality factor.

The inter-annual variability in isotopic composition is about twice larger in the cold season than in the warm season for  $\delta^{18}\text{O}$ . Different patterns of inter-annual to multi-decadal variations appear in the instrumental temperature data (see section 3.1) and ice core  $\delta^{18}\text{O}$  records (Fig 5) emerge for the cold versus the warm season.

The  $\delta\text{D}$  and  $\delta^{18}\text{O}$  values are highly correlated ( $r = 0.99$ ) on a sample to sample scale so hereafter we use the  $\delta^{18}\text{O}$  information for the dating and comparison with the other parameters. The slope between  $\delta^{18}\text{O}$  and  $\delta\text{D}$  is 8.03 on sample to sample scale and 7.9 on a seasonal scale without any significant difference between the two seasons.

No significant (R squared is insignificant at  $p < 0.05$ ) centennial trend is identified in the cold-/warm season  $\delta^{18}\text{O}$ , nor in the cold/warm season accumulation rate or deuterium excess. We observe large variations in  $\delta^{18}\text{O}$  with high and variable values in the early 20<sup>th</sup> century, lower and more stable values in the 1940s-1960s, and a step increase in the 1970s with another level. These variations are coherent in both seasons as well as in annual means but are not reflected in the meteorological observations. There is also an increase of  $\delta^{18}\text{O}$  in the last two decades in both seasons in regard to the 1970s-1980s values but the absolute values of  $\delta^{18}\text{O}$  are close to the multiannual seasonal averages (Table 3). The highest decadal values of  $\delta^{18}\text{O}$  in both seasons are observed in 1912-1920. While a recent warming trend is observed in the regional meteorological data (in warm season), it is much less prominent in the ice core  $\delta^{18}\text{O}$  record, suggesting a divergence between  $\delta^{18}\text{O}$  and regional temperature. One of the possible explanations for this feature is the post-depositional change of the isotopic composition. But we do not expect a significant influence of the post-depositional processes because of the high snow accumulation rate. The highest  $\delta^{18}\text{O}$  values for a single year correspond to the warm periods of 1984 and 1928, two years for which no unusual feature is identified from meteorological observations. The highest snow accumulation rate (fig. 9) is observed in both

seasons of 2010, in coherence with the meteorological precipitation data, and also corresponding with a record low winter NAO index.

Our deuterium excess record (fig. 2b) does not depict any robust seasonal variation. Moreover, the distribution of deuterium excess as a function of  $\delta^{18}\text{O}$  does not display any clear structure. By contrast, deuterium excess is weakly positively correlated with the accumulation rate during the warm season ( $r = 0.31$ ,  $p < 0.05$ ). This finding is consistent with the GNIP data in the region that show no link between  $\delta^{18}\text{O}$  and deuterium excess. The smoothed values of deuterium excess have prominent cycles with a period of about 25 years that are synchronous in both seasons (fig. 6). Deuterium excess is highly sensitive to surface humidity, which itself is very different and depends on the arrival of maritime air masses or dry continental air masses. This may add to the complexity of the deuterium excess signal (Pfahl and Wernli, 2008).

**3.3 Comparison of ice core records with regional meteorological data**

We compared the ice core data with the regional meteorological data and the large-scale modes of variability. The result of the correlation analysis is summarized in Table 4. Multiannual variations of the parameters are shown in fig. 9 for the cold season and in fig. 10 for the warm season.

We found no significant correlation between the ice core  $\delta^{18}\text{O}$  record and regional temperature, neither with the reanalysis data, nor with the observation data, when using the whole period. A significant correlation ( $r = 0.44$ ,  $p < 0.05$ ) emerges for warm season data, when calculated for the period since 1984. The slope for this period is 0.6 per mille per  $^{\circ}\text{C}$ . We also repeated our linear correlation analysis using precipitation weighted temperature, and obtained the same results. The precipitation weighted temperature was calculated using daily meteorological data. We used data from two stations: Klukhorskyy Pereval (as a representative of the southern stations) and Mineralnye Vody (as a representative of the northern stations).

Obviously, the above inferences strongly depend on the uncertainties of the timescale used. If one concedes that the error of the timescale could be significantly greater than  $\pm 2$  year, quite different conclusions may be reached by adjusting the scale of the  $\delta^{18}\text{O}$  and T records against each other. For instance, by contracting the  $\delta^{18}\text{O}$  record by 8 years with respect to the initial timescale in Figs 9 and 10, one would find much better correlation between  $\delta^{18}\text{O}$  and temperature, thus reaching the conclusion that the local temperature is the main driver of the  $\delta^{18}\text{O}$  variability. However, based on various experimental evidences, as discussed in the dating section, we argue that the timescale developed for the Elbrus ice core is accurate within  $\pm 2$  years. Therefore, the most realistic conclusion of those that can be drawn from the data obtained is that the temperature is weakly correlated with the  $\delta^{18}\text{O}$ , and that this correlation is unstable in time.

We also did not find any statistically significant correlations when we compared 3-, 5-, 7-years running means of these parameters. This result implies that the isotopic composition at Elbrus is controlled by both local and regional factors such as changes in moisture sources. The possibilities for accurate reconstructions of past temperatures are therefore limited. For more accurate investigation of the  $\delta^{18}\text{O}$  – temperature relation on-site experiments and subsequent modeling is required.

Our results are comparable to those obtained in the Alps by Mariani et al. (2014) for the Fiescherhorn glacier where the authors found significant, though weak, correlation between temperature and  $\delta^{18}\text{O}$ . However for the Elbrus ice core this correlation was found in the warm season only.

Another research performed in the Alps by Bohleber et al. (2013) revealed significant correlation of modified local temperature and the ice core isotopic composition at a decadal scale. The authors also report that there are some periods of correlation absence. The main finding is that for the periods of less than 25 years the difference between the modified dataset according to the authors' method and original dataset temperature is crucial, but for longer periods the two temperature datasets are close to each other. That conclusion implies that the isotopic composition reflects the local temperature in the high mountain regions to a limited extent. It seems to be impossible to calculate the modified temperature for the Caucasus region according to the methods described by Bohleber et al. (2013) because of the relatively short and sparse original datasets.

The seasonal accumulation rate is seasonal layer thickness corrected for densification using the density profile from Mikhaleenko et al. (2015) and for the layer thinning due to glacier flow using the Nye model (Nye, 1963; Dansgaard and Johnsen, 1969). It is linked to the precipitation rate on the stations situated south of the Caucasus in both seasons ( $r = 0.49$ ), and even more closely related to precipitation from Klukhorski Pereval station ( $r = 0.63$  for both seasons). We therefore establish a linear regression model for the period 1966-2013, and use this methodology to reconstruct past precipitation rates for the Klukhorskiy Pereval station (1914-1965), when meteorological records are not reliable or unavailable. The reconstructed records are shown on fig. 9 and 10 for the cold and warm seasons respectively. We found no significant trend in the reconstructed precipitation values. Even so, these results may be useful for validation of regional climate models and water resource assessment.

Calculation of the seasonal cycle of precipitation isotopic composition using the LMDZiso model (Risi et al., 2010) do not correspond to the results obtained from the ice core in absolute values or in amplitude (Fig. S5). This can be explained by a complicated relief of the region that strongly influences the isotopic composition, but it is not taken into account in the model. Also, in summer, Elbrus is in a local convective precipitation system that is not included in the model.

### 3.4 Comparison of ice core records with large-scale modes of variability

We did not find any statistically significant correlations between ice cores data and large scale modes of variability when using the mean annual values. We present the results of calculations in the table 4. We report a weak though significant ( $p < 0.05$ ) negative correlation ( $r = -0.18$ ) between the ice core accumulation rate record and NAO in the cold season. Moreover, the year of extremely high accumulation in both seasons (2010) coincides with an extremely low NAO winter index. The role of NAO in regional climate had also been evidenced by Shahgedanova et al. (2005) for the mass-balance of the Djankuat glacier situated in 30 km south-east of Elbrus for the period of 1967-2001. Interestingly, the accumulation

record is related to the variability of regional precipitation, but the latter is not significantly related to the NAO. This may suggest different influences of large-scale atmospheric circulation on precipitation at lower versus higher elevations.

~~For the cold season, the ice core  $\delta^{18}\text{O}$  record shows a~~ positive correlation with the NAO index ( $r = 0.41$ ), while the NAO index is negatively correlated with regional temperature ( $r = -0.42$ ). It also contradicts the findings of Baldini et al (2008) who, based on the GNIP low elevation dataset, extrapolated a negative correlation between the  $\delta^{18}\text{O}$  of precipitation and the NAO in this region. This finding also suggests different drivers of temperature and  $\delta^{18}\text{O}$  at low and higher elevation. We propose the following explanation for this correlation. During the positive NAO phase, the predominant moisture source for the Caucasus precipitation is the Mediterranean. During the negative NAO phase the moisture source is the Atlantic. In the first case the precipitation  $\delta^{18}\text{O}$  preserved in the ice core is higher because of the higher initial sea water isotopic composition (Gat et al., 1996) and the shorter distillation pathway. The continental recycling of moisture (Eltahir and Bras, 1996) also influences the water isotopic composition. Due to this process the  $\delta^{18}\text{O}$  values became lower while the  $d$  values increase (Aemisegger et al., 2014), which is observed in our ice core data. In the opposite situation the initial water isotopic composition is close to 0 ‰ (Frew et al., 2000) and the distillation pathway is longer which leads to lower values of precipitation  $\delta^{18}\text{O}$ .

We explored the links between the ice core parameters ( $\delta^{18}\text{O}$ , accumulation rate) with the NCP index and found no significant correlation in winter, or in summer despite the significant correlation between the NCP and local temperature and precipitation. A possible explanation may be that the NCP pattern only affects low elevation regional climate but not high elevation climate.

No significant correlation was identified between deuterium excess and indices of large scale modes of variability. So far, no regional or large-scale climate signal could be identified in Elbrus deuterium excess. Further investigations using back trajectories and diagnoses of moisture source and evaporation characteristics will be needed to explore further the drivers of this second-order isotopic parameter.

#### 4 Conclusion

We found no persistent link between ice cores  $\delta^{18}\text{O}$  and temperature on an interannual scale, a common feature emerging from non-polar ice cores (e.g. Mariani et al., 2014). This finding is not an artefact of high elevation versus low elevation difference, because the variability of the regional temperature stack used for this comparison is in good agreement with the variability of the temperature at the drilling site as observed by the local AWS.

Our ice core records depict large decadal variations in  $\delta^{18}\text{O}$  with high and variable values in the late 19<sup>th</sup>-early 20<sup>th</sup> centuries, lower and more stable values in the 1940s-1960s, followed by a step increase in the 1970s. No unusual recent change is detected in the isotopic composition or in the accumulation rate record, in contrast with the observed warming trend from

656 regional meteorological data. The accumulation rate appears significantly related to the NAO index coherently with the  
657 earlier results for the Djankuat glacier (Shahgedanova et al. 2005).  
658 Based on regional meteorological information and trajectory analyses, the main moisture source is situated not far from the  
659 drilling site in the warm season, and consists of evaporation from the Black Sea and continental evapotranspiration. Changes  
660 in regional temperature during the warm season may affect the initial vapour isotopic composition as well as the atmospheric  
661 distillation processes, including convective activity, in a complex way. This may explain the significant, albeit non  
662 persistent, correlation of summer  $\delta^{18}\text{O}$  and temperature. Cold season moisture sources appear more variable geographically,  
663 with potential contributions from the North Atlantic to the Mediterranean regions. Changes in moisture origin appear to  
664 dominate in regional temperature-driven distillation processes. As a result, the isotopic composition of the ice cores appears  
665 mostly related to characteristics of large-scale atmosphere circulation such as the NAO index. The changes in moisture  
666 origin also influence the deuterium excess parameter, which does not have any prominent seasonal variations.  
667 Our data can be used in atmospheric models equipped with water stable isotopes, for instance to assess their ability to  
668 resolve NAO–water isotope relationships (Langebroek et al., 2011, Casado et al., 2014). The accumulation rate at the drilling  
669 site is significantly correlated with the precipitation rate and gives information about precipitation variability before the  
670 beginning of meteorological observations.

671  
672 **Acknowledgements**

673  
674 The research was supported by the RFBR grants 14-05-31102 mol. a and 17-05-00771 a. The analytical procedure ensuring a  
675 high accuracy of isotope data obtained at CERL was elaborated with financial support from the Russian Science Foundation,  
676 grant 14-27-00030. The study of dust layers was conducted with the support of RFBR grant 14-05-00137. The measurement  
677 of the samples in IAEA was conducted according to research contracts 16184/R0, and 16795. This research work was  
678 conducted in the framework of the International Associated Laboratory (LIA) “Climate and Environments from Ice  
679 Archives” 2012–2016, linking several Russian and French laboratories and institutes. We thank Obbe Tuinenburg and Jean-  
680 Louis Bonne for the back trajectory calculations. We thank Alice Lagnado for improving the English. We are grateful to four  
681 anonymous reviewers and the Editor Professor Hou Shugui for their comments, which helped to improve the paper.

682  
683 **References**

684 Aemisegger F., Pfahl S., Sodemann H., Lehner I., Seneviratne S.I., Wernli H.: Deuterium excess as a proxy for continental  
685 moisture recycling and plant transpiration, *Atmos. Chem. Phys.*, 14, 4029–4054, doi:10.5194/acp-14-4029-2014, 2014.  
686 Baldini L.M., McDermott F., Foley A.M., Baldini J.U.L.: Spatial variability in the European winter precipitation  $\delta^{18}\text{O}$ -NAO  
687 relationship: Implications for reconstructing NAO-mode climate variability in the Holocene, *Geophys. Res. Letters*. 35,  
688 doi:10.1029/2007GL032027, L04709, 2008.

Отформатировано: Английский (США)

Отформатировано: надстрочные

689 Bohleber P., Wagenbach D., Schonher W., Bohm R.: To what extent do water isotope record from low accumulation Alpine  
690 ice cores reproduce instrumental temperature series? Tellus B, 65, 20148, doi:10.3402/tellusb.v65i0.20148, 2013.

691 Brunetti M., Kutiel H.: The relevance of the North-Sea Caspian Pattern (NCP) in explaining temperature variability in  
692 Europe and the Mediterranean, Nat. Hazards Earth Syst. Sci., 11, 2881–2888, doi:10.5194/nhess-11-2881-2011, 2011.

693 Casado M, Ortega P., Masson-Delmotte V., Risi C., Swingedouw D., Daux V., Genty D., Maignan F., Solomina O., Vinter  
694 B., Viovy N., Yiou P.: Impact of precipitation intermittency on NAO-temperature records, Clim. Past, 9, 871-886,  
695 doi:10.5194/cp-9-871-2013, 2013.

696 Comas-Bru, L., McDermott, F. and Werner, M. (2016): The effect of the East Atlantic pattern on the precipitation  $\delta^{18}\text{O}$ -  
697 NAO relationship in Europe, Climate Dynamics, doi: 10.1007/s00382-015-2950-1

698 Dansgaard, W.: Stable isotopes in precipitation, Tellus, 16(4), 436–468, 1964

699 Dansgaard, W., Johnsen, S.J.: A flow model and a time scale for the ice core from Camp Century, Greenland, J. Glaciol.,  
700 8(53), 215–223, 1969.

701 Draxler, R.R., and Hess G.D.: An overview of the HYSPLIT\_4 modeling system of trajectories, dispersion, and deposition.  
702 Aust. Meteor. Mag., 47, 295-308, 1998.

703 Ekaykin A.A., Lipenkov V.Ya.: Formation of the ice core isotopic composition, Physics of ice core records II, ed. T.Hondoh,  
704 Low Temperature Science, 68, Hokkaido Univ. Press, Sapporo, 299-314, 2009.

705 Elizbarashvili E.Sh., Elizbarashvili, M.R., Tatishvili, M.E., Elizbarashvili, Sh.E., Elizbarashvili, R.Sh.: Meskhiya Air  
706 temperature trends in Georgia under global warming conditions, Russ. Meteorol. Hydrol., 38, 234–238, 2013.

707 Eltahir E.A.B., Bras R.L.: Precipitation recycling, Reviews of Geophysics 34, 3, 367-378, doi: 8755-12 09/96/96 RG-01927,  
708 1996

709 Forster C., Stohl A., Siebert P.: Parametrization of convective transport in a lagrangian particle dispersion model and its  
710 evaluation, Journ. of Applied Meteorology and Climatology, 46 (4), 403–422, doi:10.1175/JAM2470.1, 2007.

711 Frew, R., Dennis, P.F., Heywood K.J., Meredith M.P., and Boswell S.M.: The oxygen isotope composition of water masses  
712 in the northern North Atlantic, Deep Sea Research Part I: Oceanographic Research Papers, 47, 12, 2265-2286,  
713 doi:10.1016/S0967-0637(00)00023-6, 2000.

714 Gat, J.R., Shemesh, A., Tziperman, E., Hecht, A., Georgopoulos, D., and Basturk, O.: The stable isotope composition of  
715 waters of the eastern Mediterranean Sea, J. Geophysical Res., 101, 3, 6441-6451, doi: 10.1029/95JC02829, 1996.

716 Johnsen S., Clausen H.B., Cuffey K.M., Hoffmann G., Schwander J., Creys T.: Diffusion of stable isotopes in polar firn and  
717 ice: the isotope effect in firn diffusion, Physics of Ice Core Records, Edited by T. Hondoh, Hokkaido University Press,  
718 Sapporo, 121–140, 2000.

719 Kalnay, E., Kanamitsu, M., Kistler, R., Collins, W., Deaven, D., Gandin, L., Iredell, M., Saha, S., White, G., Woollen, J.,  
720 Zhu, Y., Leetmaa, A., Reynolds, B., Chelliah, M., Ebisuzaki, W., Higgins, W., Janowiak, J., Mo, K. C., Ropelewski, C.,  
721 Wang, J., Jenne, R., Joseph, D.: The NCEP/NCAR 40-Year Reanalysis Project, Bulletin of the American Meteorological  
722 Society, 77, 3, 437-472, doi: 10.1175/1520-0477(1996)077<0437:TNYRP>2.0.CO;2, 1996.

Отформатировано: надстрочные

- Код поля изменен
- Код поля изменен
- Код поля изменен
- Код поля изменен
- Код поля изменен
- Код поля изменен
- Код поля изменен
- Код поля изменен
- Код поля изменен
- Код поля изменен
- Код поля изменен
- Код поля изменен
- Код поля изменен
- Код поля изменен
- Код поля изменен
- Код поля изменен
- Код поля изменен
- Код поля изменен
- Код поля изменен
- Код поля изменен

723 Kozachek A.V., Ekaykin A.A., Mikhaleiko V.N., Lipenkov V.Y., Kutuzov S.S.: Isotopic composition of ice cores obtained  
724 at the Elbrus Western Plateau, *Ice and Snow*, 55, 4, doi: 10.15356/2076-6734-2015-4-35-49, 35-49, 2015 (in Russian with  
725 English summary)

726 Kutuzov, S., Shahgedanova, M., Mikhaleiko, V., Lavrentiev, I. and Kemp, S.: Desert dust deposition on Mt. Elbrus,  
727 Caucasus Mountains, Russia in 2009–2012 as recorded in snow and shallow ice core: high-resolution “provenancing”,  
728 transport patterns, physical properties and soluble ionic composition, *The Cryosphere*, 7(5), 1481–1498, doi:10.5194/tc-7-  
729 1481-2013, 2013.

730 Langebroek, P. M.; Werner, M.; Lohmann, G.: Climate information imprinted in oxygen-isotopic composition of  
731 precipitation in Europe, *Earth and Planetary Science Letters*, 311, 1, 144–154, 10.1016/j.epsl.2011.08.049, 2011.

732 Mariani I., Eichler A., Jenk M., Brönnimann S., Auchmann R., Leuenberger M.C., Schwikowski M.: Temperature and  
733 precipitation signal in two Alpine ice cores over the period 1961–2001, *Clim. Past*, 10, 1093–1108, doi:10.5194/cp-10-1093-  
734 2014, 2014.

735 Mikhaleiko V., Sokratov S., Kutuzov S., Ginot P., Legrand M., Preunkert S., Lavrentiev I., Kozachek A., Ekaykin A., Faïn  
736 X., Lim S., Schotterer U., Lipenkov V., Toropov P.: Investigation of a deep ice core from the Elbrus western plateau, the  
737 Caucasus, Russia, *The Cryosphere*, 9, 2253–2270, doi:10.5194/tc-9-2253-2015, 2015.

738 Mikhaleiko, V.N., Kuruzov, S.S., Lavrentiev, I.I., Kunakhovich, M.G., and Thompson, L.G.: Issledovanie zapadnogo  
739 lednikovogo plato Elbrusa: rezul'taty i perspektivy (Western Elbrus Plateau studies: results and perspectives), *Materialy*  
740 *glyatsiologicheskikh issledovaniy* (Data Glaciol. Stud.), (99), 185–190, 2005 (in Russian with English summary)

741 Mountain Research Initiative EDW Working Group: Elevation-dependent warming in mountain regions of the world, *Nature*  
742 *Climate Change*, 5, 424–430, doi:10.1038/nclimate2563, 2015.

743 Panagiotopoulos F., Shahgedanova M., Steffenson D.B.: A review of Northern Hemisphere winter time teleconnection patterns, *J. Phys. IV France*, 12, doi: 10.1051/jp4:20020450,  
744 2002.

745 Persson, A., P. L. Langen, P. Ditlevsen, B. M. Vinther: The influence of precipitation weighting on interannual variability of  
746 stable water isotopes in Greenland, *J. Geophys. Res.*, 116, D20120, doi:10.1029/2010JD015517, 2011.

747 Pfahl S. and Wernli H.: Air parcel trajectory analysis of stable isotopes in water vapor in the eastern Mediterranean, *J.*  
748 *Geophys. Res.*, 113, D20104, doi:10.1029/2008JD009839, 2008.

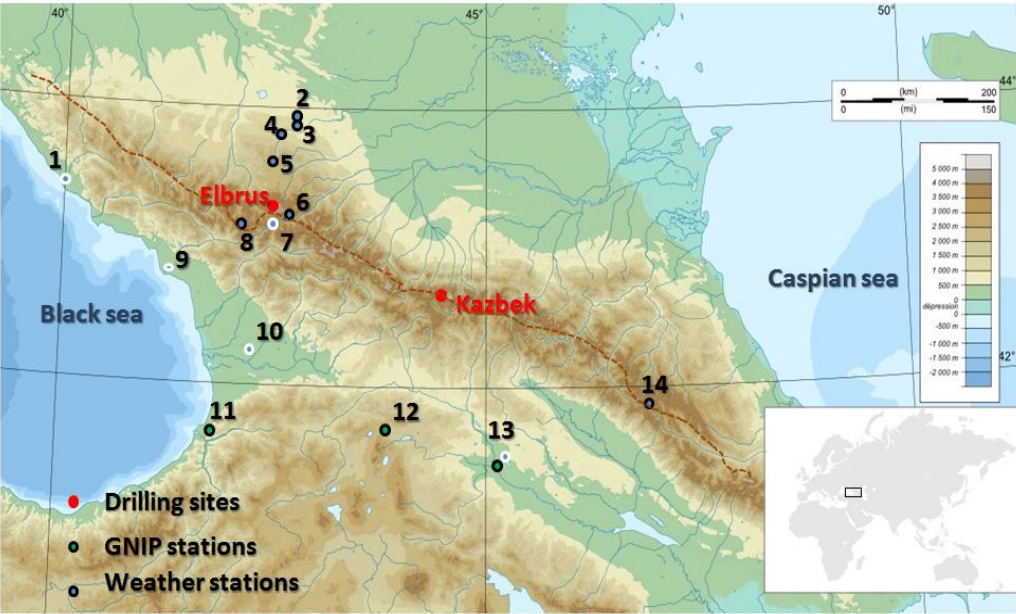
749 Risi C., Bony S., Vimeux F., Jouzel J.: Water stable isotopes in the LMDZ4 general circulation model: Model evaluation for  
750 present-day and past climate and implications to climatic interpretation of tropical isotopic records, *Journal of Geophysical*  
751 *Research*, 115, D12118, doi:10.1029/2009JD013255, 2010.

752 Rolph, G.D., Real-time Environmental Applications and Display sYstem (READY) Website (<http://ready.arl.noaa.gov>).  
753 NOAA Air Resources Laboratory, Silver Spring, MD, 2016.

754 Shahgedanova M., Nosenko G., Kutuzov S., Rototaeva O., and Khromova T.: Deglaciation of the Caucasus Mountains,  
755 Russia/Georgia, in the 21st century observed with ASTER satellite imagery and aerial photography, *The Cryosphere*, 8(6),  
756 2367–2379, doi:10.5194/tc-8-2367-2014, 2014.

757 Shahgedanova M., Stokes C., Gurney S., Popovnin V.: Interactions between mass balance, atmospheric circulation, and  
 758 recent climate change on the Djankuat Glacier, Caucasus Mountains, Russia, *Journ. of Geophys. Research*, 110, D04108,  
 759 doi:10.1029/2004JD005213, 2005.  
 760 Stein, A.F., Draxler, R.R., Rolph, G.D., Stunder, B.J.B., Cohen, M.D., and Ngan, F.: NOAA's HYSPLIT atmospheric  
 761 transport and dispersion modeling system, *Bull. Amer. Meteor. Soc.*, 96, 2059-2077, doi: 10.1175/BAMS-D-14-00110.1,  
 762 2015.  
 763 Stoffel M., Khodri M., Corona C., Guillet S., Poulain V., Bekki S., Guiot J., Luckman B.H., Oppenheimer C., Lebas N.,  
 764 Beniston M., and Masson-Delmotte V.: Estimates of volcanic-induced cooling in the Northern Hemisphere over the past  
 765 1,500 years, *Nature Geoscience* 8, 784–788, doi:10.1038/ngeo2526, 2015.  
 766 Stohl A., Thompson D.J.: A density correction for lagrangian particle dispersion models, *Boundary Layer Meteorology*, 90  
 767 (1), 155–167, doi:10.1023/A:1001741110696, 1999.  
 768 Tielidze L.G.: Glacier change over the last century, Caucasus Mountains, Georgia, observed from old topographical maps,  
 769 Landsat and ASTER satellite imagery, *The Cryosphere*, 10, 713-725, doi:10.5194/tc-10-713-2016, 2016.  
 770 Toropov P.A., Mikhaleiko V.N., Kutuzov S.S., Morozova P.A., Shestakova A.A.: Temperature and radiation regime of  
 771 glaciers on slopes of the Mount Elbrus in the ablation period over last 65 years, *Ice and Snow*, 56(1), 5-19,  
 772 doi:10.15356/2076-6734-2016-1-5-19, 2016 (In Russian with English summary).  
 773 Tsushima A., Matoba S., Shiraiwa T., Okamoto S., Sasaki H., Solie D.J., Yoshikawa K.: Reconstruction of recent climate  
 774 change in Alaska from the Aurora Peak ice core, central Alaska, *Clim. Past*, 11, 217–226, doi:10.5194/cp-11-217-2015,  
 775 2015.  
 776 Vinther, B. M., S. J. Johnsen, K. K. Andersen, H. B. Clausen, A. W. Hansen: NAO signal recorded in the stable isotopes of  
 777 Greenland ice cores, *Geophys. Res. Lett.*, 30(7), 1387, doi:10.1029/2002GL016193, 2003  
 778 Vinther B.M., Jones P.D., Briffa K.B., Clausen H.B., Andersen K.K., Dahl-Jensen D., Johnsen S.J.: Climatic signals in  
 779 multiple highly resolved stable isotopes records from Greenland, *Quat. Sci. Rev.* 29 (3-4), 522-538, 2010  
 780 Volodicheva, N.: The Caucasus, in: *The Physical geography of Northern Eurasia*, edited by: Shahgedanova, M., Oxford  
 781 University Press, Oxford, 350–376, 2002  
 782 .

783 Figures  
784  
785



786  
787  
788 Fig. 1: Map showing the region around Elbrus (black rectangle in the world's map in the lower right corner), with shading  
789 indicating elevation (m above sea level). Drilling sites are indicated with red filled circles, GNIP stations as green filled circles, and  
790 meteorological stations as blue dots. Stations situated to the south of the Main Caucasus Ridge according to the precipitation cycle  
791 pattern are shown using a blue dot with white outside circle and the stations situated to the north are displayed with black outside  
792 circle (see text for ~~the~~ details). The brown dotted line shows the border between two types of precipitation seasonal cycles. The  
793 number of the various stations refers to Table 1 for their detailed description.  
794

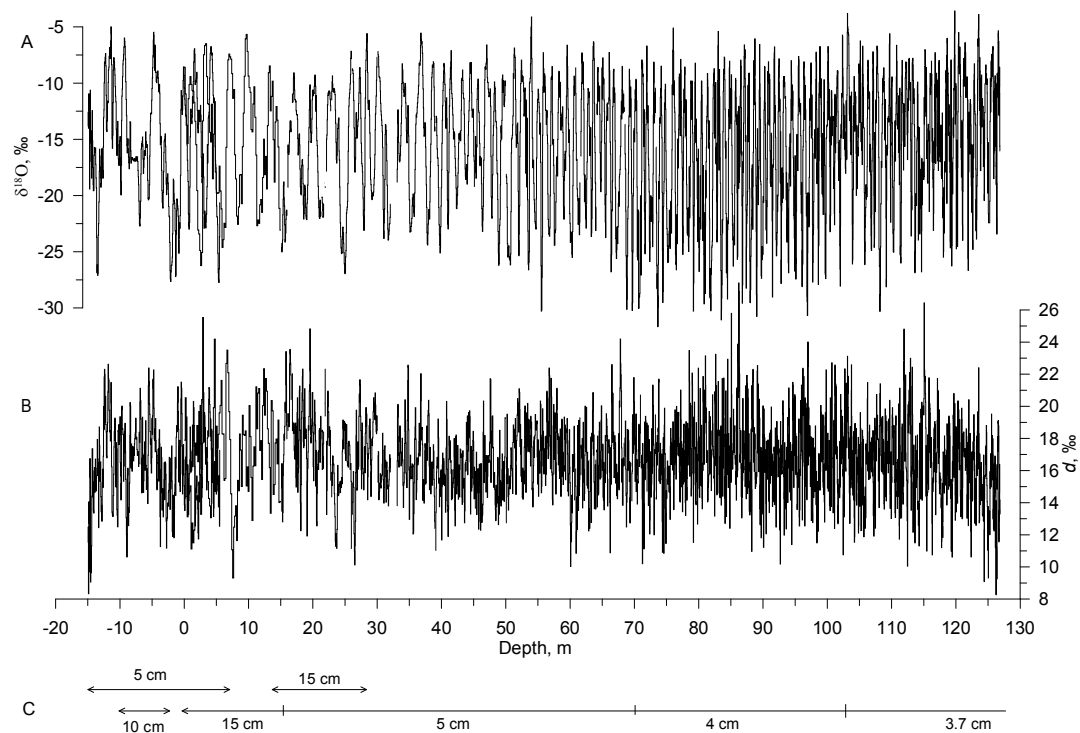


**Fig. 2. Vertical profile of  $\delta^{18}\text{O}$  (A), deuterium excess (B), and the number of the ice core as well as sampling resolution (C). 0 m depth corresponds to the surface of 2009.**

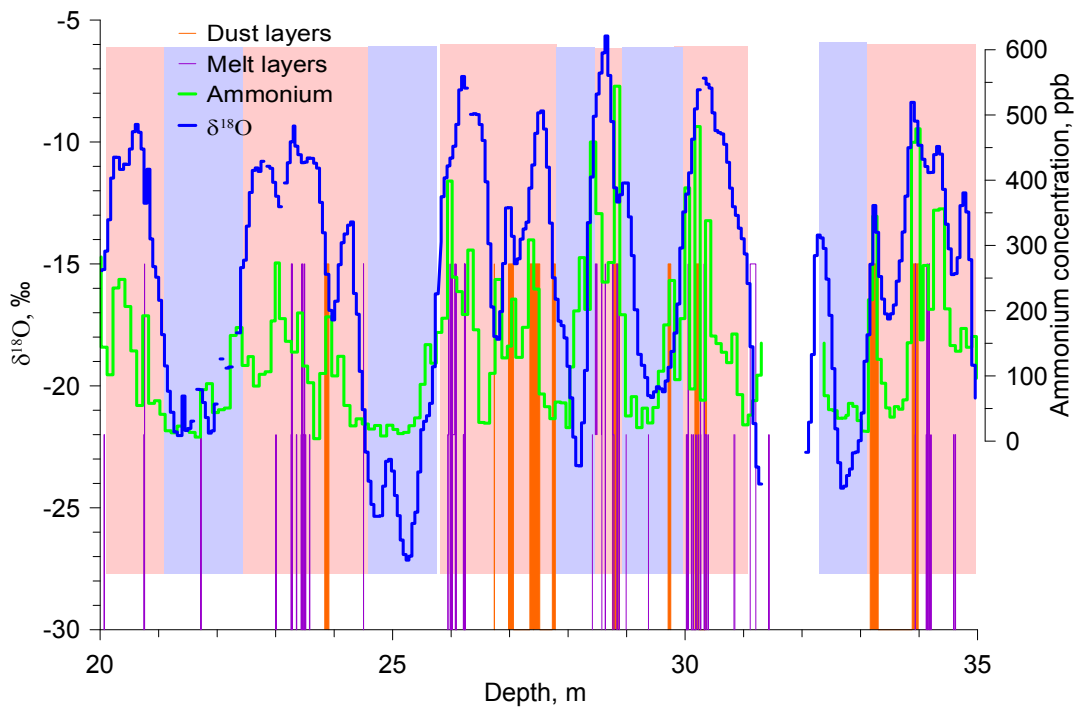
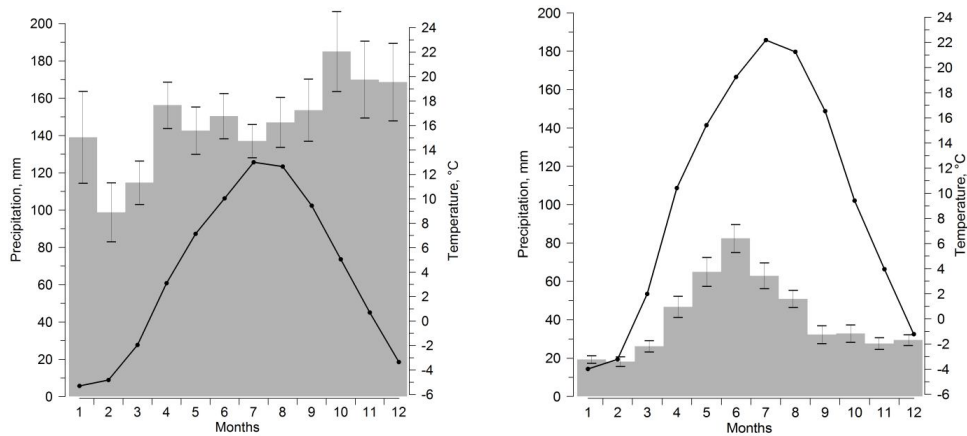


Fig. 3: Illustration of the scheme used to identify warm and cold half-years (respectively indicated by the light red and light blue shaded areas) based on the deviation of the mean  $\delta^{18}\text{O}$  values from the long-term average value. The purple lines depict the melt layers observed in the core, dust layers are shown in orange, and the ammonium concentration graph (Mikhaleenko et al., 2015) is in green.



**Fig. 4: Average seasonal cycle of temperature (black dots and line) and precipitation (grey bars) calculated over 1966-1990 period, a) for the Klukhorskyy Pereval station (illustrating the lack of a distinct seasonal cycle in precipitation south of the Caucasus) and b) for the Mineralnye Vody station (illustrating the clear seasonal cycle in precipitation seen in stations north of the Caucasus). Error bars (SEM) are shown for the interannual standard deviation of the monthly precipitation rate while the same error bars for the temperature are dimensionless at the scale of the graph.**

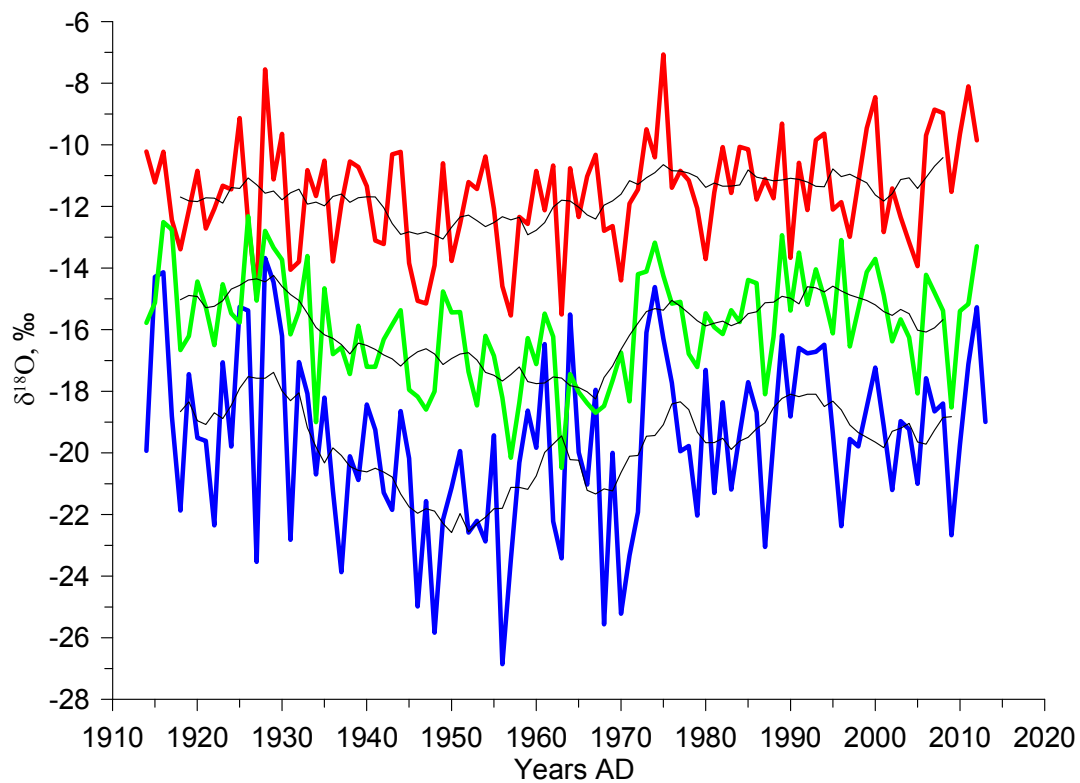


Fig. 5: Annual variations of  $\delta^{18}\text{O}$  in warm season (red line), in cold season (blue line), and annual means (green line). Thin black lines show 10-year running means of these parameters.

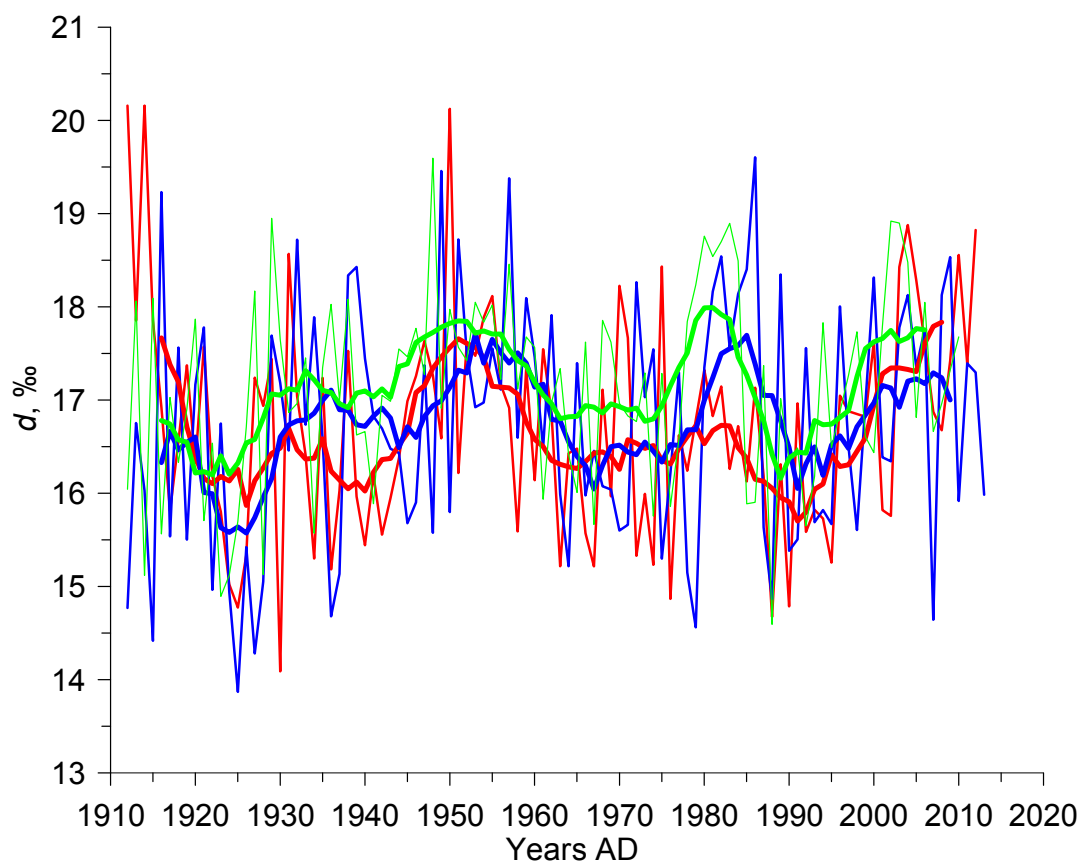
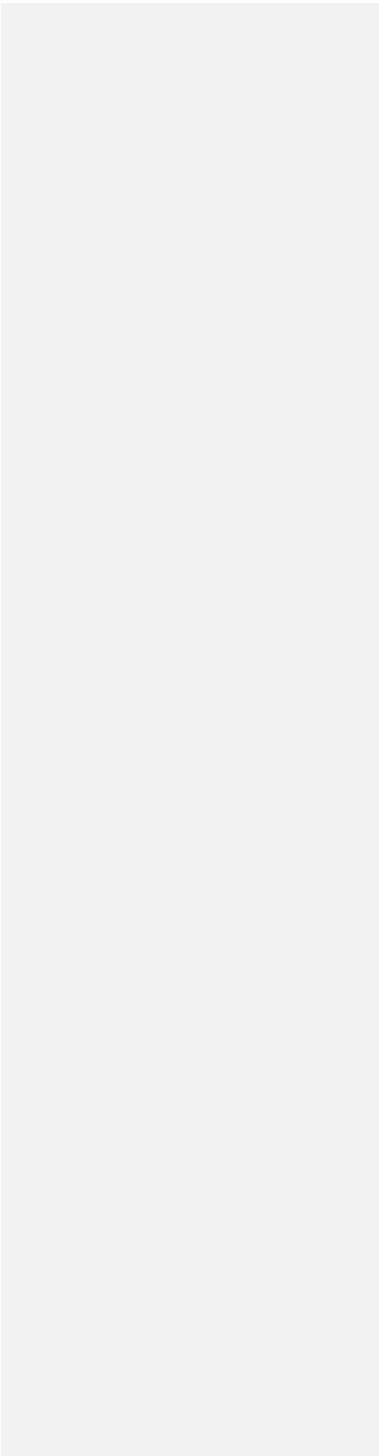
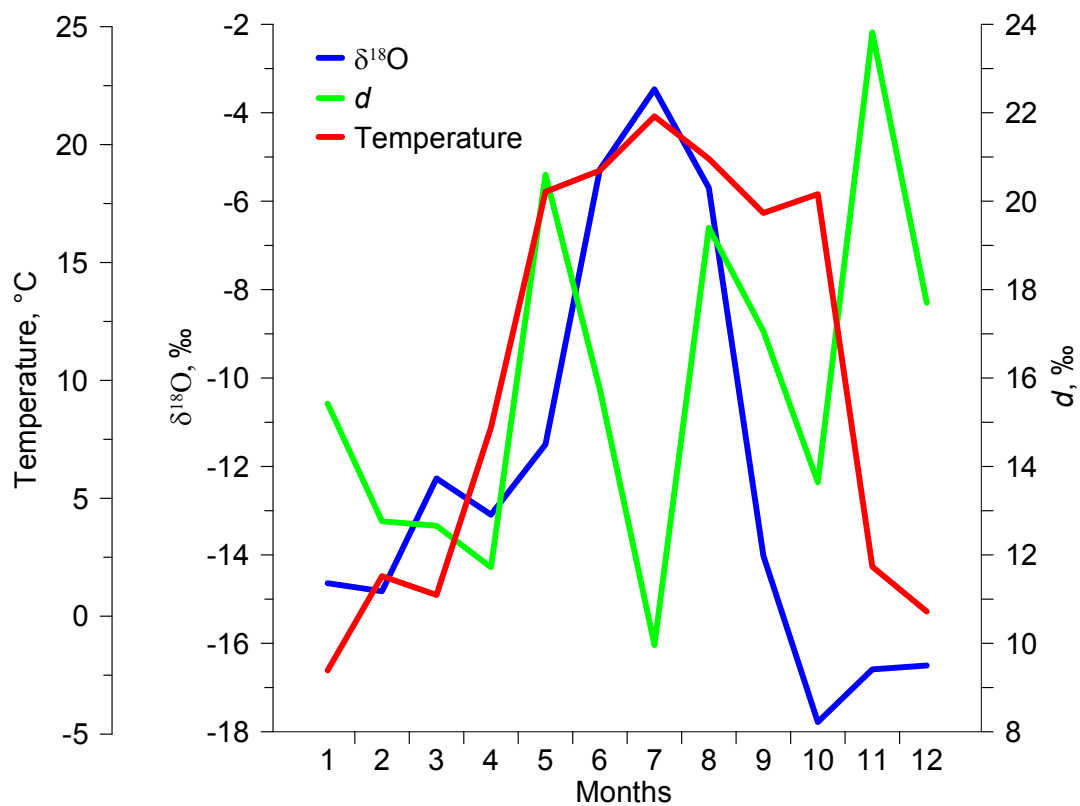


Fig. 6: Annual variations of deuterium excess in warm season (red line), in cold season (blue line), and mean annual values (green line). Thick lines show the 10-year smoothed values and the thin ones display the raw values.





Отформатировано: Шрифт: 9 пт,  
полужирный

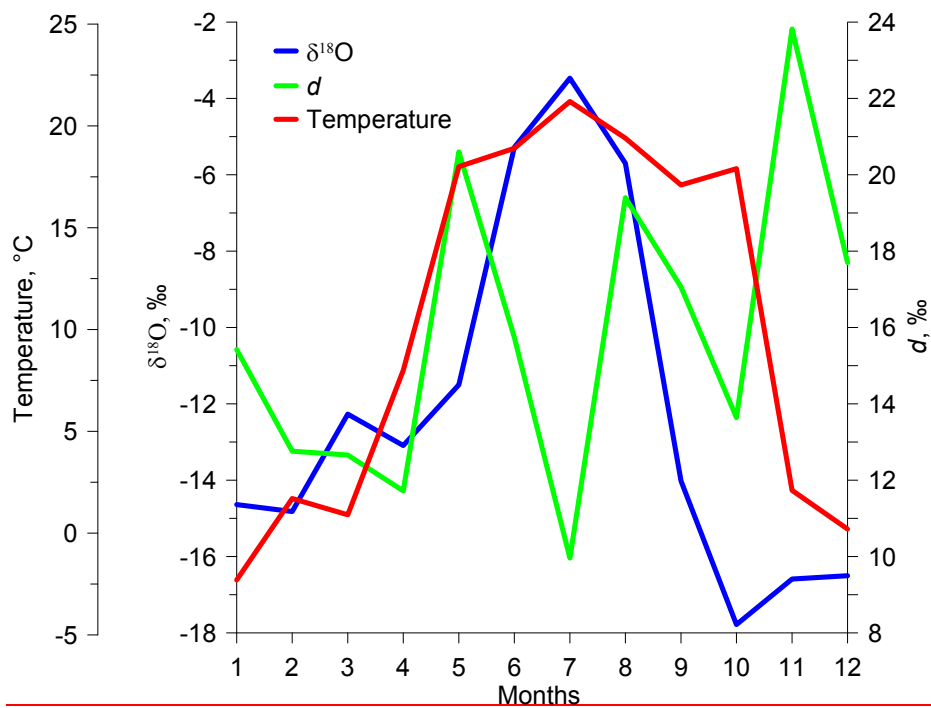
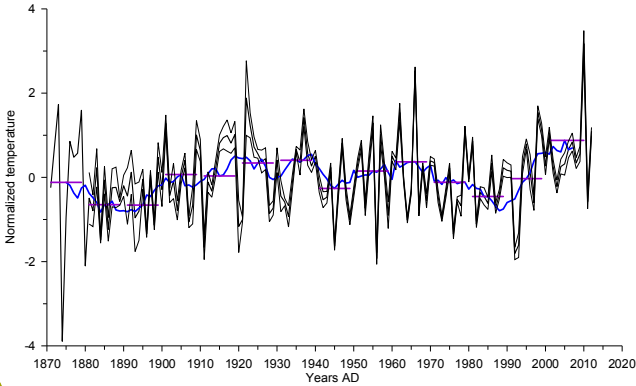
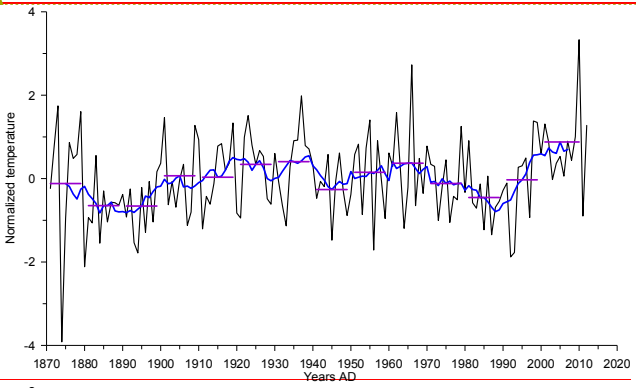


Fig. 7: Monthly  $\delta^{18}\text{O}$  (blue line),  $d$  (green line) and air temperature (red line) data at Bakuriani GNIP station in 2009 (see Table 1 for information on station and Fig. 1 for its location). Note that there is no clear seasonal cycle in deuterium excess, in contrast with  $\delta^{18}\text{O}$  showing maximum values in summer and minimum values in winter.

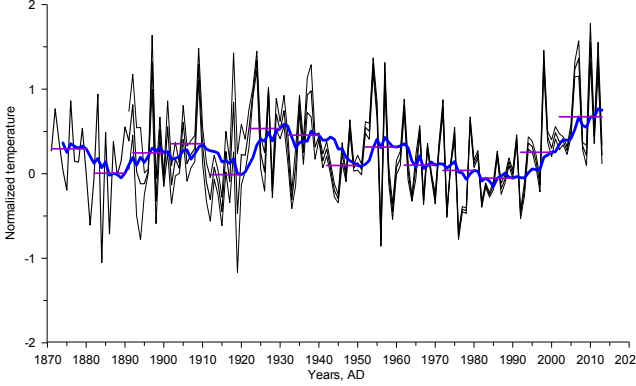
829



830



831



Отформатировано: Шрифт: 9 пт, полужирный

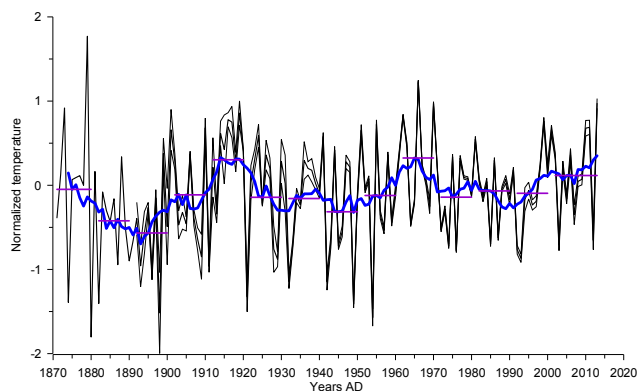
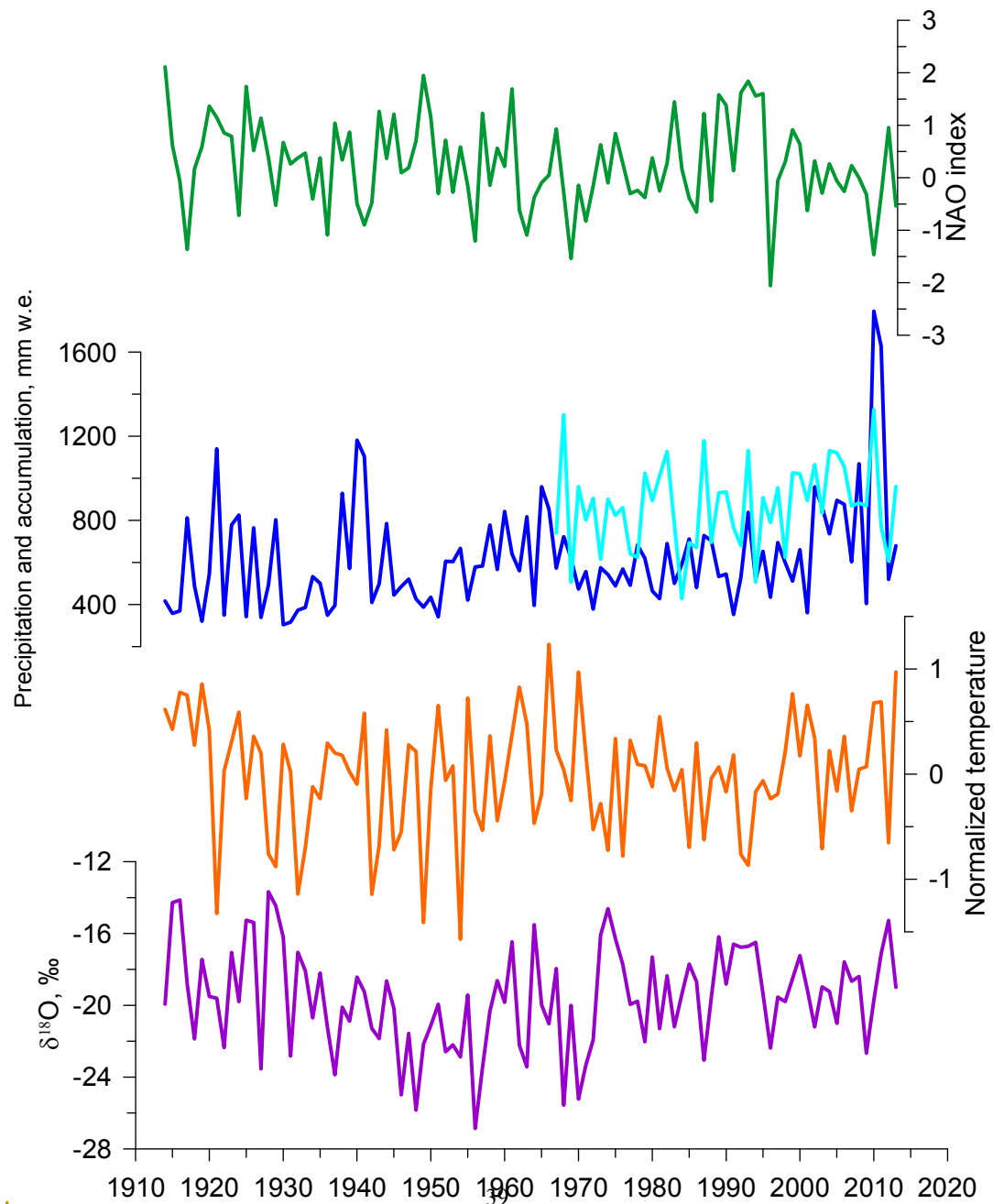


Fig. 8: Normalized regional temperature record based on meteorological data, with respect to the reference period 1966-1990, expressed as annual anomalies ( $^{\circ}\text{C}$ ). The thin lines illustrate the standard deviation across the individual records after accounting for the lapse rate from Fig. S3, the blue line shows a 10 year running mean and the horizontal purple line demonstrates the decadal mean value. The upper panel shows the annual means, the middle panel shows the warm season, and the lower panel shows the cold season—the upper panel for the annual means, middle panel for the warm season, and the lower panel for the cold season.

Отформатировано: Английский (США)



Отформатировано: Шрифт: 9 пт,  
полужирный

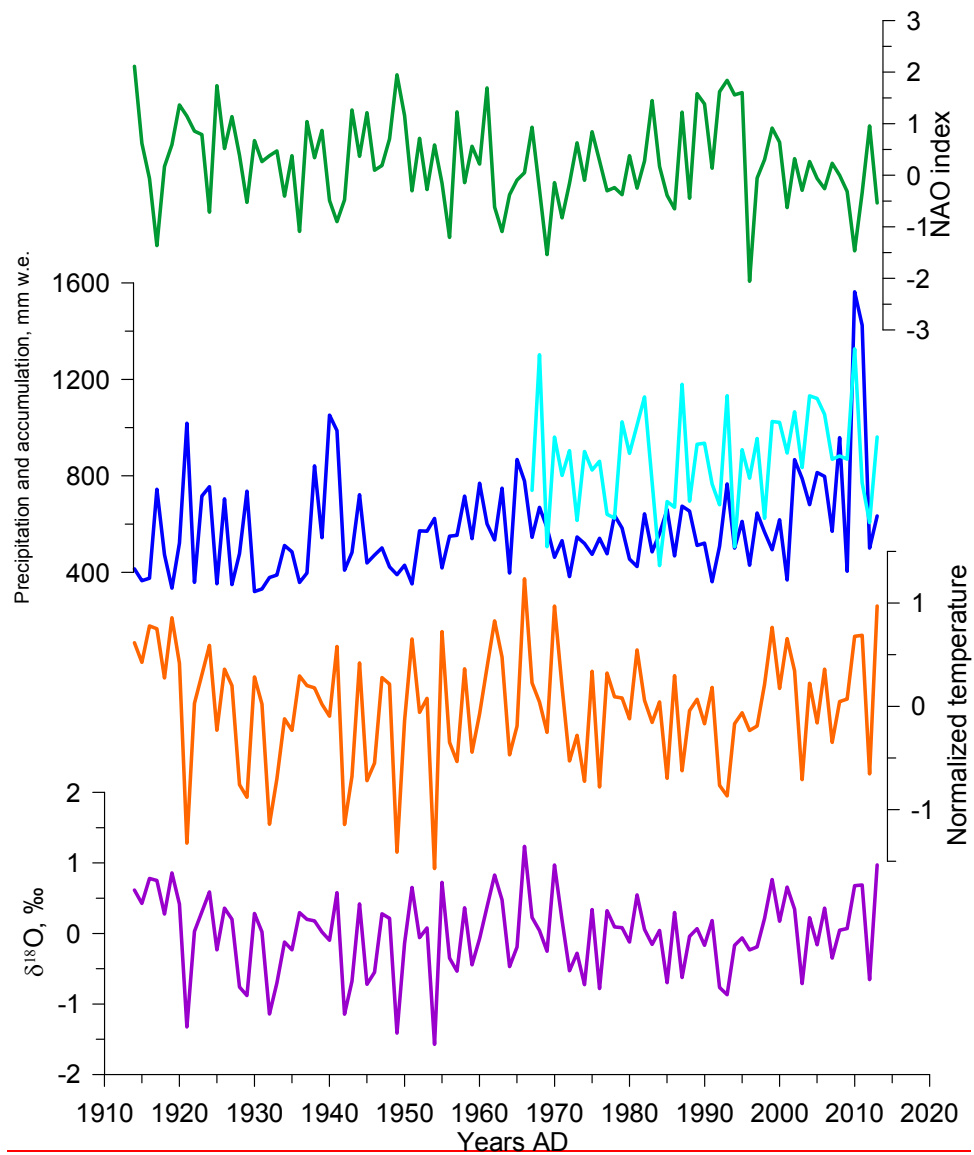


Fig. 9: Comparison of the ice core record with instrumental regional climate information, for the cold season:  $\delta^{18}\text{O}$  composite (purple), temperature at the drilling site calculated from the lapse rate (brown), precipitation at the Klukhorskij Pereval station (light blue) as well as the ice core accumulation estimate (dark blue) and NAO index (green).

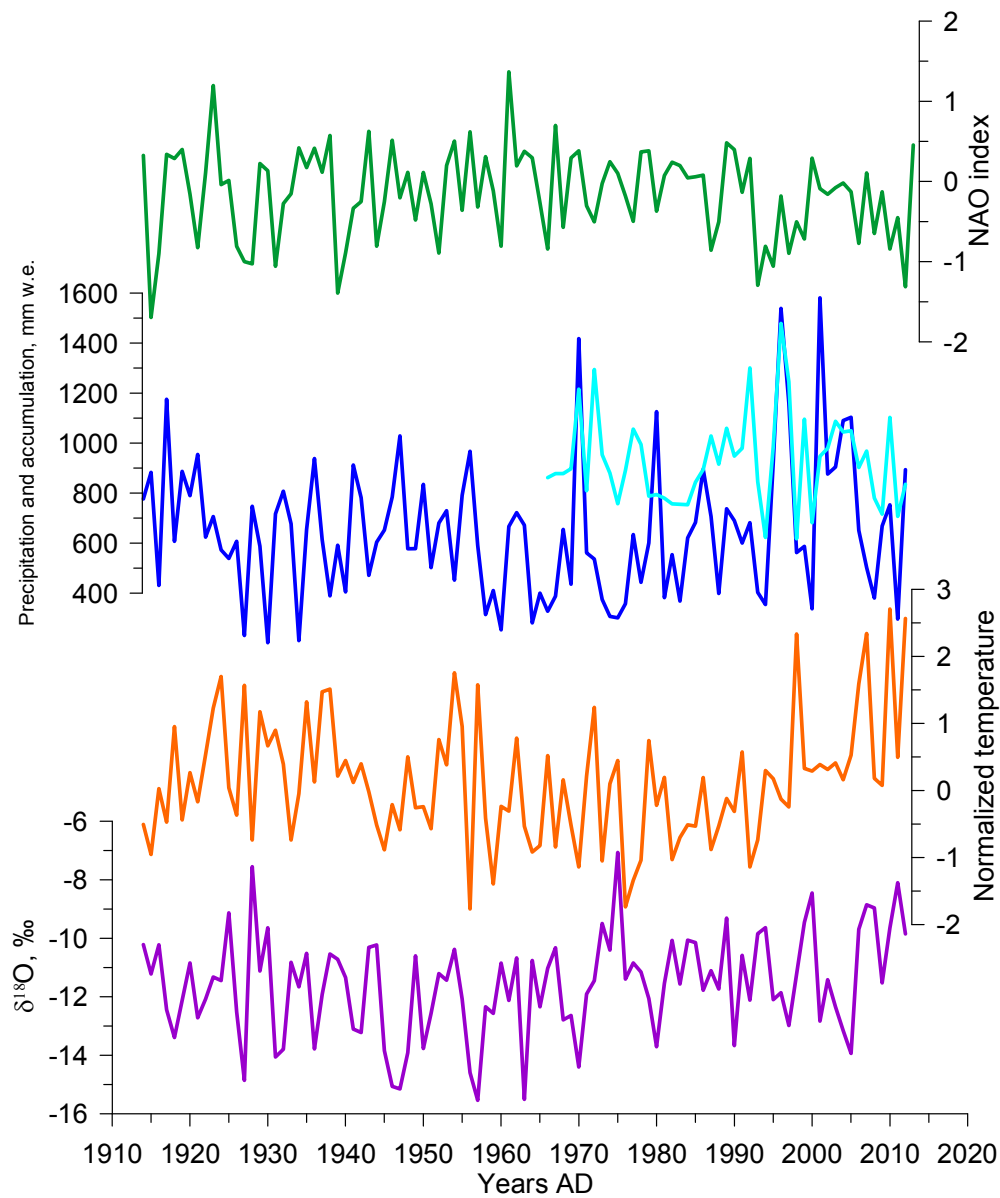


Fig. 10: Same as fig. 9 but for the warm season.

848 **Table 1: Description of meteorological and instrumental data used in the paper**

Data type	Number on map (Fig. 1)	Location/Name	Altitude a.s.l.	Time span	Data source
Meteorological observations (temperature, precipitation rate) with daily resolution	1	Sochi	57 m	1871-present	www.meteo.ru
	2	Mineralnye Vody	315 m	1938-present	
	3	Kislovodsk	943 m	1940-present	
	4	Pyatigorsk	538 m	1891-1997	
	5	Shadzhatmaz	2070 m	1959-present	
	6	Terskol	2133 m	1951-2005	
	7	Klukhorsk <sup>iy</sup> Pereval	2037 m	1959-present	
	8	Teberda	1550 m	1956-2005	
	9	Sukhumi	75 m	1904-1988	
	10	Samtredia	24 m	1936-1992	
	13	Tbilisi	448 m	1881-1992	
	14	Sulak	2927 m	1930-present	
	15	Mestia	1417 m	1930-1991	
GNIP data	11	Batumi	32 m	1980-1990	<a href="http://www-naweb.iaea.org/napc/ih/IHS_resources_gnip.html">http://www-naweb.iaea.org/napc/ih/IHS_resources_gnip.html</a>
	12	Bakuriani	1700 m	2008-2009	
	13	Tbilisi	448 m	2008-2009	
Circulation indices	n/a	NAO	n/a	1821-present	Vinter et al., 2009 <a href="https://crudata.uea.ac.uk/~timo/datasets/naoi.htm">https://crudata.uea.ac.uk/~timo/datasets/naoi.htm</a>
			n/a	1950-present	<a href="http://www.cpc.ncep.noaa.gov/products/precip/CWlink/">http://www.cpc.ncep.noaa.gov/products/precip/CWlink/</a>
	n/a	NCP	n/a	1948-present	
	n/a	AO	n/a	1950-present	
Reanalysis daily temperature	n/a	NCEP	500 mb level	1948-present	<a href="http://www.esrl.noaa.gov/psd/data/gridded/data.ncep.reanalysis.html">http://www.esrl.noaa.gov/psd/data/gridded/data.ncep.reanalysis.html</a> Kalnay et al., 1996
Back trajectories	n/a	Flexpart	n/a	2002-2009	Forster et al., 2007, Stohl et al., 2009
	n/a	Hysplit	n/a	1948-present	Draxler, 1999, Stein et al., 2015, Rolph, 2016
	n/a	LMDZiso	n/a	n/a	Risi et al., 2010

850  
851  
852  
853  
854

Table 2: Correlation coefficients between meteorological data and indices of large-scale modes of variability (statistically significant coefficients at  $p < 0.05$  are highlighted in bold). The period of calculation and number of data points (n) for each coefficient are shown in brackets.

Annual mean	Temperature	P south*	P north*
NAO	<b>-0.24</b> (1914-2013, n=100)	-0.24 (1966-2013, n=48)	-0.03 (1966-2013, n=48)
AO	<b>-0.34</b> (1950-2013, n=64)	-0.06 (1966-2013, n=48)	0.02 (1966-2013, n=48)
NCP	<b>-0.55</b> (1948-2013, n=66)	0.26 (1966-2013, n=48)	0.26 (1966-2013, n=48)
Warm season			
NAO	<b>-0.47</b> (1914-2013, n=100)	0.23 (1966-2013, n=48)	0.03 (1966-2013, n=48)
AO	-0.11 (1950-2013, n=64)	0.08 (1966-2013, n=48)	0.14 (1966-2013, n=48)
NCP	<b>-0.50</b> (1948-2013, n=66)	<b>0.34</b> (1966-2013, n=48)	<b>0.34</b> (1966-2013, n=48)
Cold season			
NAO	<b>-0.41</b> (1914-2013, n=100)	0.04 (1966-2013, n=48)	0.26 (1966-2013, n=48)
AO	<b>-0.40</b> (1950-2013, n=64)	0.14 (1966-2013, n=48)	<b>0.37</b> (1966-2013, n=48)
NCP	<b>-0.77</b> (1948-2013, n=66)	0.25 (1966-2013, n=48)	<b>0.33</b> (1966-2013, n=48)

855  
856  
857  
858  
859  
860  
861

\*P south – precipitation rate at the weather stations to the South from the Caucasus, P north – precipitation rate at the weather stations to the North from the Caucasus.

863  
864

**Table 3: Mean characteristics of the Elbrus ice core records, calculated for the period from 1914 to 2013.**

Annual means	$\delta^{18}\text{O}$ , ‰	$\delta\text{D}$ , ‰	$d$ , ‰	Accumulation rate (m w.e./year)
Mean	$-15.90$	$-110.10$	17.11	1.29
Standard deviation	1.76	14.03	1.02	0.44
<b>Cold season</b>				
Mean	$-19.61$	$-140.11$	16.59	0.71
Standard deviation	2.81	22.54	2.11	0.36
<b>Warm season</b>				
Mean	$-11.58$	$-75.97$	16.69	0.65
Standard deviation	1.75	13.98	1.14	0.27

865  
866  
867

Table 4. Correlation coefficients between ice core data, meteorological data and indices of large-scale modes of variability (statistically significant coefficients at  $p < 0.05$  are highlighted in bold). The period of calculation and number of data points (n) for each coefficient is shown in brackets.

Annual means	$\delta^{18}\text{O}$	Accumulation	$d$	NAO	AO	NCP
$T, ^\circ\text{C}$	$-0.01$ (1914-2013, n=100)	$0.16$ (1914-2013, n=100)	$0.00$ (1914-2013, n=100)	$-0.24$ (1914-2013, n=100)	$-0.34$ (1950-2013, n=64)	$-0.55$ (1948-2013, n=66)
P north*	$-0.30$ (1966-2013, n=48)	<b>0.36</b> (1966-2013, n=48)	$0.17$ (1966-2013, n=48)	$-0.03$ (1966-2013, n=48)	$-0.03$ (1966-2013, n=48)	$0.27$ (1966-2013, n=48)
P south*	$0.06$ (1966-2013, n=48)	<b>0.52</b> (1966-2013, n=48)	$0.07$ (1966-2013, n=48)	$-0.24$ (1966-2013, n=48)	$-0.06$ (1966-2013, n=48)	$0.18$ (1966-2013, n=48)
$\delta^{18}\text{O}$		$-0.20$ (1914-2013, n=100)	$-0.06$ (1914-2013, n=100)	$0.07$ (1914-2013, n=100)	<b>0.41</b> (1950-2013, n=64)	$0.11$ (1948-2013, n=66)
Accumulation			<b>0.21</b> (1914-2013, n=100)	$-0.29$ (1914-2013, n=100)	$-0.29$ (1950-2013, n=64)	$-0.03$ (1948-2013, n=66)
$d$				$-0.08$ (1914-2013, n=100)	$-0.26$ (1950-2013, n=64)	$-0.14$ (1948-2013, n=66)
Warm season	$\delta^{18}\text{O}$	Accumulation	$d$	NAO	AO	NCP
$T, ^\circ\text{C}$	$0.13$ (1914-2013, n=100)	$-0.04$ (1914-2013, n=100)	<b>0.20</b> (1914-2013, n=100)	$-0.02$ (1914-2013, n=100)	$-0.10$ (1950-2013, n=64)	$-0.51$ (1948-2013, n=66)
P north*	$0.01$ (1966-2013, n=48)	$0.16$ (1966-2013, n=48)	$0.09$ (1966-2013, n=48)	$0.13$ (1966-2013, n=48)	$-0.14$ (1966-2013, n=48)	$0.18$ (1966-2013, n=48)
P south*	$-0.27$ (1966-2013, n=48)	<b>0.49</b> (1966-2013, n=48)	$-0.02$ (1966-2013, n=48)	$-0.01$ (1966-2013, n=48)	$0.07$ (1966-2013, n=48)	<b>0.34</b> (1966-2013, n=48)
$\delta^{18}\text{O}$		$-0.42$ (1914-2013, n=100)	$-0.05$ (1914-2013, n=100)	$-0.08$ (1914-2013, n=100)	$0.16$ (1950-2013, n=64)	$0.00$ (1948-2013, n=66)
Accumulation			<b>0.31</b> (1914-2013, n=100)	$0.00$ (1914-2013, n=100)	$0.09$ (1950-2013, n=64)	$0.00$ (1948-2013, n=66)
$d$				$0.00$ (1914-2013, n=100)	$-0.01$ (1950-2013, n=64)	$-0.14$ (1948-2013, n=66)
Cold season	$\delta^{18}\text{O}$	Accumulation	$d$	NAO	AO	NCP
$T, ^\circ\text{C}$	$-0.09$ (1914-2013, n=100)	$0.11$ (1914-2013, n=100)	$-0.15$ (1914-2013, n=100)	$-0.30$ (1914-2013, n=100)	$-0.45$ (1950-2013, n=64)	$-0.79$ (1948-2013, n=66)
P north*	$0.20$ (1966-2013, n=48)	$0.21$ (1966-2013, n=48)	$-0.12$ (1966-2013, n=48)	<b>0.51</b> (1966-2013, n=48)	<b>0.37</b> (1966-2013, n=48)	$0.23$ (1966-2013, n=48)
P south*	$-0.30$ (1966-2013, n=48)	<b>0.37</b> (1966-2013, n=48)	$-0.13$ (1966-2013, n=48)	$0.26$ (1966-2013, n=48)	$0.14$ (1966-2013, n=48)	$0.25$ (1966-2013, n=48)
$\delta^{18}\text{O}$		$0.05$ (1914-2013, n=100)	$0.02$ (1914-2013, n=100)	<b>0.41</b> (1914-2013, n=100)	<b>0.41</b> (1950-2013, n=64)	$0.19$ (1948-2013, n=66)
Accumulation			$0.07$ (1914-2013, n=100)	$-0.18$ (1914-2013, n=100)	$-0.15$ (1950-2013, n=64)	$0.18$ (1948-2013, n=66)
$d$				$-0.06$ (1914-2013, n=100)	$-0.01$ (1950-2013, n=64)	$0.11$ (1948-2013, n=66)

\*P south – precipitation rate at the weather stations to the South from the Caucasus, P north – precipitation rate at the weather stations to the North from the Caucasus.

Отформатировано: Шрифт: не полужирный

Отформатировано: По центру

Отформатировано: По центру

Отформатировано: По центру

Отформатировано: По центру

Отформатировано: По центру

Отформатировано: По центру

Отформатировано: По центру

Отформатировано: По центру

Отформатировано: По центру

Отформатировано: По центру

Отформатировано: По центру

Отформатировано: По центру

Отформатировано: По центру

868  
869